metabolites

MDPI

Article

The Over-Irradiation Metabolite Derivative, 24-Hydroxylumister-ol$_3$, Reduces UV-Induced Damage in Skin

Warusavithana Gunawardena Manori De Silva [1,†], Bianca Yuko McCarthy [1,†], Jeremy Han [1], Chen Yang [1], Andrew J. A. Holland [2], Harvey Stern [3,4], Katie Marie Dixon [1], Edith Kai Yan Tang [5], Robert Charles Tuckey [5], Mark Stephen Rybchyn [1] and Rebecca Sara Mason [1,6,*]

1 School of Medical Sciences and Bosch Institute, The University of Sydney, Sydney, NSW 2006, Australia; wdes3780@uni.sydney.edu.au (W.G.M.D.S.); bianca.mccarthy@lubrizol.com (B.Y.M.); j.han@garvan.org.au (J.H.); ayang@cmri.org.au (C.Y.); katie.dixon@sydney.edu.au (K.M.D.)
2 Douglas Cohen Department of Paediatric Surgery, The Children's Hospital at Westmead Clinical School, The Faculty of Medicine and Health, The University of Sydney, Sydney, NSW 2006, Australia; andrew.holland@health.nsw.gov.au
3 Department of Plastic and Constructive Surgery, The Royal Prince Alfred Hospital, Sydney, NSW 2050, Australia; hstern@bigpond.net.au
4 Strathfield Private Hospital, Sydney, NSW 2042, Australia
5 School of Molecular Sciences, The University of Western Australia, Perth, WA 6009, Australia; edith.tang@uwa.edu.au (E.K.Y.T.); robert.tuckey@uwa.edu.au (R.C.T.)
6 School of Life and Environmental Sciences, Charles Perkins Centre, University of Sydney, Sydney, NSW 2006, Australia
* Correspondence: rebecca.mason@sydney.edu.au; Tel.: +61-421-619-783
† These authors contributed equally to this work.

Abstract: The hormonal form of vitamin D_3, 1,25(OH)$_2$D$_3$, reduces UV-induced DNA damage. UV exposure initiates pre-vitamin D_3 production in the skin, and continued UV exposure photoisomerizes pre-vitamin D_3 to produce "over-irradiation products" such as lumisterol$_3$ (L_3). Cytochrome P450 side-chain cleavage enzyme (CYP11A1) in skin catalyzes the conversion of L_3 to produce three main derivatives: 24-hydroxy-L_3 [24(OH)L_3], 22-hydroxy-L_3 [22(OH)L_3], and 20,22-dihydroxy-L_3 [20,22(OH)L_3]. The current study investigated the photoprotective properties of the major over-irradiation metabolite, 24(OH)L_3, in human primary keratinocytes and human skin explants. The results indicated that treatment immediately after UV with either 24(OH)L_3 or 1,25(OH)$_2$D$_3$ reduced UV-induced cyclobutane pyrimidine dimers and oxidative DNA damage, with similar concentration response curves in keratinocytes, although in skin explants, 1,25(OH)$_2$D$_3$ was more potent. The reductions in DNA damage by both compounds were, at least in part, the result of increased DNA repair through increased energy availability via increased glycolysis, as well as increased DNA damage recognition proteins in the nucleotide excision repair pathway. Reductions in UV-induced DNA photolesions by either compound occurred in the presence of lower reactive oxygen species. The results indicated that under in vitro and ex vivo conditions, 24(OH)L_3 provided photoprotection against UV damage similar to that of 1,25(OH)$_2$D$_3$.

Keywords: 1,25(OH)$_2$D$_3$,1,25-dihydroxyvitamin D_3; 24(OH)L_3; 24-hydroxy-lumisterol$_3$; 8OHdG; 8-hydroxy-2′-deoxyguanosine; ATP; adenosine tri-phosphate; CPD; cyclobutane pyrimidine dimer; CYP11A; cytochrome P450 side-chain cleavage enzyme 11A; ROS; reactive oxygen species; siRNA; small interfering RNA; UVR; ultraviolet radiation; UDS; unscheduled DNA synthesis; VDR; vitamin D receptor; XPA; xeroderma pigmentosum complementation group A; XPC; xeroderma pigmentosum complementation group C

check for updates

Citation: De Silva, W.G.M.; McCarthy, B.Y.; Han, J.; Yang, C.; Holland, A.J.A.; Stern, H.; Dixon, K.M.; Tang, E.K.Y.; Tuckey, R.C.; Rybchyn, M.S.; et al. The Over-Irradiation Metabolite Derivative, 24-Hydroxylumister-ol$_3$, Reduces UV-Induced Damage in Skin. *Metabolites* **2023**, *13*, 775. https://doi.org/10.3390/metabo13070775

Academic Editor: Qi Wu and Dewei Jiang

Received: 21 April 2023
Revised: 13 June 2023
Accepted: 16 June 2023
Published: 21 June 2023

Copyright: © 2023 by the authors. Licensee MDPI, Basel, Switzerland. This article is an open access article distributed under the terms and conditions of the Creative Commons Attribution (CC BY) license (https://creativecommons.org/licenses/by/4.0/).

1. Introduction

While sunlight clearly has many positive benefits, the detrimental effects of sun exposure on skin were first proposed by Paul Gerson Unna in 1894 [1]. Studies since then have

shown that UVB radiation in sunlight induces harmful effects such as sunburn, DNA damage [2,3], cell-mediated immunosuppression [4], mutations, and photocarcinogenesis [5]. UVA also contributes to DNA damage and photo-aging [6,7]. The harmful effects of UVA and UVB both contribute to photocarcinogenesis.

When sequential pyrimidine bases of the same DNA strand absorb UV photons, this direct DNA damage results in dimeric photolesions [3,8]. *Cis-syn* cyclobutane pyrimidine dimers (CPDs), mostly formed between 5–6 bonds of adjacent thymine and cytosine bases, are the most common lesions found. Of these, thymine dimers (T–T) are the majority and are formed in numbers directly proportional to the total of all types of CPDs [9]. Thymine–cytosine dimers and cytosine–cytosine dimers have been shown to be highly mutagenic [2,10].

Indirect DNA damage such as oxidative damage to DNA purine bases contributes to mutagenesis, aging, pathological conditions, and photocarcinogenesis [11–13]. Indirect DNA damage is mainly caused by free radicals, reactive oxygen species (ROS) [14,15], and reactive nitrogen species (RNS) [16]. UV exposure increases ROS production and depletes antioxidants, resulting in an increased ROS to antioxidant ratio, considered to be the main contributor to the formation of oxidative photolesions [17–20]. Types of ROS include singlet oxygen ($^1O_2$) [15], hydroxyl radical, hydrogen peroxide, and the superoxide anion [21,22]. These free radicals mainly target guanine in the DNA, and this oxidation reaction produces the main photolesion, 8-oxo-7, 8-dihydro-2′-deoxyguanosine (8-OHdG) [23–27]. ROS contributes to gene mutations [28], DNA strand breakage [29], aging [30], mitochondrial damage [31], structural damage (organelle membranes), and functional protein damage (including DNA repair proteins), all of which may promote carcinogenesis [32–35].

CPDs are repaired by the highly conserved nucleotide excision repair (NER) pathway [36–38]. Two subpathways of NER consist of transcription coupled nucleotide excision repair (TC-NER) and global genomic nucleotide excision repair (GG-NER). The major difference between these pathways lies in the initial damage recognition process. One important damage recognition protein involved in GG-NER is xeroderma pigmentosum complementation group C (XPC) protein [39–41]. XPC acts as the main damage sensor that triggers GG-NER [42,43] and is a structure-specific damage factor [44,45]. The xeroderma pigmentosum complementation group A (XPA) protein has a higher affinity for damaged DNA than undamaged DNA [46] and is vital for progression in both TC-NER and GG-NER [47].

One of the beneficial effects of UVB exposure is the biosynthesis from 7-dehydrocholesterol of pre-vitamin D_3, which at body temperature isomerizes to vitamin D_3 [48]. Skin exposed to UVB radiation converts vitamin D_3 to its hormonal form, 1,25$(OH)_2D_3$ (Figure 1) [49–51]. Several studies have shown that vitamin D metabolites reduce UV-induced DNA damage in skin cell cultures, mice, and human skin [52–57]. This reduction in DNA damage leads to reductions in skin tumors in mouse models [53,57].

Vitamin D_3 is not the only compound produced in skin from 7-dehydrocholesterol by UVB exposure. Also produced are the so-called "over-irradiation" products [58–60] (Figure 1). Continued exposure to UV photoisomerizes pre-vitamin D_3 to produce biologically "inactive over-irradiation products", lumisterol$_3$ and tachysterol$_3$ [61–64]. Cytochrome P450 side-chain cleavage enzyme/CYP11A1 is a mitochondrial enzyme [65], which upregulates after UVB exposure [66–68]. This enzyme catalyzes the conversion of vitamin D_3 itself to several isomers that have some photoprotective properties [69–73] and converts lumisterol$_3$ into 24-hydroxylumisterol$_3$ [24(OH)L_3], 22-hydroxylumisterol$_3$ [22(OH)L_3], and 20,22-dihydroxylumisterol$_3$ [20,22$(OH)_2L_3$] [68,72]. Lumisterol$_3$ and its hydroxyderivatives are metabolically stable in that they are not metabolized by 7-dehydrocholesterol reductase, unlike their 7-dehydrocholesterol stereoisomers [74]. The current study investigated the in vitro and ex vivo photoprotective properties on DNA damage of the over-irradiation metabolite, 24(OH)L_3.

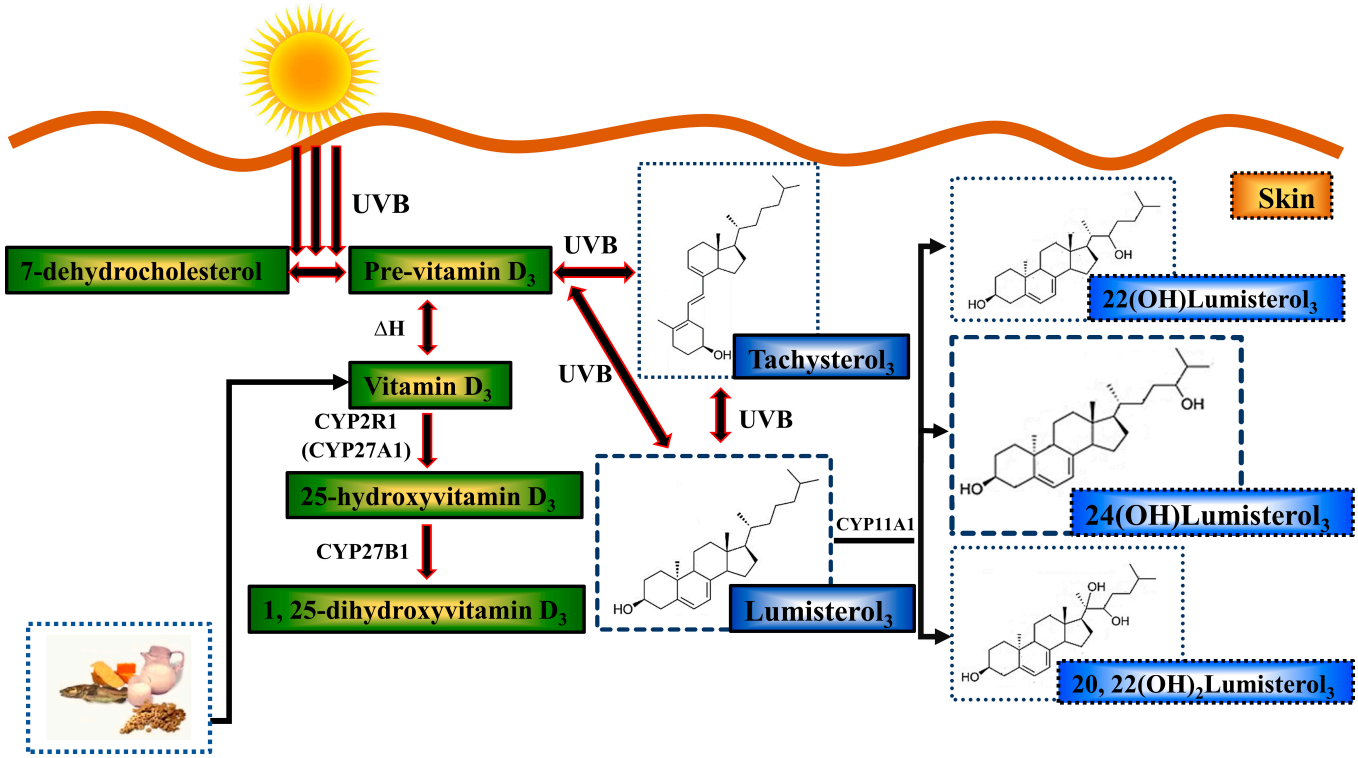


Figure 1. Biosynthesis and metabolism of vitamin D and over-irradiation products after UV radiation. When 7-dehydrocholesterol in skin absorbs UVB, it is converted to pre-vitamin D_3. Pre-vitamin D_3 thermo-isomerizes into vitamin D_3 at body temperature. Vitamin D is converted in the liver and other tissues, including skin, to 25-hydroxyvitamin D_3 by CYP2R1/CYP27A1 enzymes and then to the biologically active vitamin D hormone, 1,25-dihydroxyvitamin D_3 ($1,25(OH)_2D_3$), in the kidney and other tissues including skin by CYP27B1. Exogenous vitamin D can be acquired through food, such as fish or supplements. Continuous UVB exposure photo-isomerizes pre-vitamin D_3 to produce what used to be considered relatively biologically inactive "over-irradiation products" such as lumisterol$_3$ (L3), tachysterol$_3$, and other compounds. CYP11A1 is a cytochrome P450 enzyme found in skin which catalyzes L3 to 22(OH)lumisterol$_3$, 24(OH)lumisterol$_3$, and $20,22(OH)_2$lumisterol$_3$ as the major products. Green color shows classic vitamin D compounds. Blue color shows over-irradiation products and metabolites.

2. Materials and Methods

2.1. Cell Cultures and Skin Explants

Skin samples for keratinocyte culture or skin explant culture were harvested after obtaining written informed consent from subjects or their parents/guardians, with approval from the University of Sydney Human Ethics Committee (Reference number 2015/063).

- Keratinocytes: Keratinocytes were grown out from skin fragments [75] and cultured as previously described with minor modifications [76], in keratinocyte growth medium (KGM), which contained minimum essential medium Eagle (M0518, Sigma-Aldrich, St. Louis, MO, USA), 0.02 M sodium bicarbonate (Sigma-Aldrich, St. Louis, MO, USA), 1 mM sodium pyruvate, and 25 mM HEPES (ThermoFisher Scientific, Waltham, MA, USA) in MilliQ water at pH 7.2 (Millipore SAS, Molsheim, France). Human primary keratinocytes were cultured in KGM containing 5% (v/v) fetal calf serum (FCS) and the following supplements: 5 µg/mL transferrin, 0.4 ug/mL hydrocortisone, 1×10^{-10} M cholera toxin, 10 ng/mL Epidermal Growth Factor (EGF), 5 µg/mL insulin (all from Sigma-Aldrich, St. Louis, MO, USA), and 2×10^{-11} M 3,3,5-triiodo-L-thyronine sodium salt [77]. Keratinocytes from passages 2–5 from at least two independent donors were used in all experiments. The keratinocyte culture media was changed

to media without EGF and cholera toxin for 24 h before experiments to allow cells to become quiescent [78].

- Skin explants: Human skin explants were collected from consenting patients undergoing elective surgery at private hospitals in Sydney, Australia, and processed as previously described [56]. In brief, ice-cold sterile phosphate buffered saline (PBS) was used to transport the skin back to the laboratory. The skin was processed under aseptic conditions within 4 h of surgery. The skin was briefly washed with 4% chlorhexidine gluconate solution (Sigma-Aldrich, St. Louis, MO, USA) and then thoroughly washed with ice-cold PBS. Subcutaneous fat and debris were trimmed off to leave the epidermis and dermis only, for the study. The skin samples were dissected into 4 mm pieces with a punch biopsy tool with five biopsies prepared for each treatment. The skin samples were then prepared for UV irradiation as described below.

2.2. Solar-Simulated UV Irradiation

UV irradiation was provided by an Oriel Sol1A^{TM} 94042A 450 W solar simulator (Newport Corporation, Irvine, CA, USA) with an atmospheric attenuation filter to eliminate UVC (<290 nm). It was calibrated using the OL756 spectroradiometer (Gooch & Housego, Melbourne, FL, USA), and an IL 1700 broadband radiometer (International Light Technologies, Peabody, MA, USA) was used immediately prior to experiments to determine the UVB output, from which a calculated dose of solar-simulated UV (ssUV) was determined. This dose of UV did not increase caspase activity or decrease the total DNA and equated to approximately 4 min of sunlight at noon in October in Sydney, Australia [79]. The spectral output of this lamp as used for these experiments has been published [Figure S6 in [79]].

- Keratinocytes: Immediately prior to UV irradiation, the medium was replaced with irradiation buffer, Martinez solution containing 10 mM D-glucose (Sigma-Aldrich, St. Louis, MO, USA) without phenol red. For all keratinocyte experiments, the ssUV irradiation energy level was 400 mJ/cm^2 UVB and 3600 mJ/cm^2 UVA (4000 mJ/cm^2) [53,79].
- Skin explants: Skin biopsies were placed in ice-cold sterile colorless Martinez buffer with the epidermis facing up in a volume that was just enough to surround the tissue without submersion, for UV radiation [56]. A single dose of ssUV at 20 J/cm^2 was delivered to the skin explant samples. Sham/non-irradiated keratinocytes or skin were subjected to similar procedures but not irradiated.

2.3. 1,25(OH)$_2$D$_3$ and 24(OH)L$_3$ Treatments

The 1,25(OH)$_2$D$_3$ was from Sapphire Bioscience Pty Ltd., (Sydney, Australia). The 24(OH)L$_3$ was enzymatically synthesized using recombinant CYP11A1 and purified using procedures as previously described [72,80]. These compounds were solubilized in spectroscopic grade ethanol (Merck, Darmstadt, Germany) and added to cultures in 0.1% (v/v) ethanol. The ethanol vehicle 0.1% (v/v) was used as a control. The concentration of these compounds was determined with a Nanodrop ND-1000 Spectrophotometer (ThermoFisher Scientific, Waltham, MA, USA) immediately prior to use.

- Keratinocytes: Immediately after UV irradiation (or sham irradiation), the irradiation buffer was replaced with supplement-free keratinocyte growth medium (KGM) containing vehicle, 0.1% (v/v) ethanol, or treatments at the concentrations as indicated.
- Skin explants: Immediately after UV irradiation (or sham irradiation), the skin samples were treated with vehicle, 0.1% (v/v) ethanol, or treatments in RPMI-1640 media (Sigma-Aldrich, St. Louis, MO, USA) supplemented with 10% FCS, penicillin, and streptomycin at 37 °C.

2.4. Immunohistochemistry

The current study used an antibody detection method for thymine dimers as an index of total CPDs and antibody detection of 8-OHdG followed by image analysis. These methods produced similar results to those that detected CPDs or 8-OHdG by a specific endonuclease followed by a Comet assay [54,76]. CPDs consist of thymine–thymine,

thymine–cytosine, cytosine–thymine, or cytosine–cytosine photoproducts [81]. Using a direct assay of a combination of liquid chromatography and tandem mass spectrometry to determine the different fractions of dimer photoproducts after UV, thymine dimers were found to be the most abundant, eightfold higher than other photolesions and correlated with the number of other dimers [9,82]. Thus, thymine dimers are routinely used as a measure of the total CPDs.

- Keratinocytes:

CPDs and 8-OHdG: At the end of the incubation period after UV exposure (3 h or the period mentioned for the experiment), the keratinocytes were rinsed with PBS after incubation, and the keratinocytes were fixed with ice-cold 100% methanol (Sigma-Aldrich, St. Louis, MO, USA) at −20 °C for 10 min. Cells were extensively washed with MilliQ water and air dried overnight prior to immunohistochemistry, which was carried out as previously described [55], with minor modifications. Endogenous peroxidase activity was blocked by 1% (*v*/*v*) H_2O_2 (ThermoFisher Scientific, Waltham, MA, USA) in PBS for 5 min followed by two MilliQ water washes. Antigen retrieval was carried out in several steps. Nuclear DNA was denatured with 70 mM NaOH (Sigma-Aldrich, St. Louis, MO, USA) in 70% ethanol for 2 min. Proteolytic digestion was achieved with 1 µg/mL Proteinase K (Sigma-Aldrich, St. Louis, MO, USA) in 0.1 mM $CaCl_2$ for 5 min for CPD detection and 10 min for 8-OHdG detection followed by two MilliQ water washes. Non-specific antibody binding was inhibited by treating cells with 50% (*v*/*v*) horse serum (Sigma-Aldrich, St. Louis, MO, USA) in PBS (blocker) for 1 h. The cells were incubated with primary antibody for 60 min at room temperature, either mouse monoclonal anti-thymine dimer at 5 µg/mL (Sigma-Aldrich, St. Louis, MO, USA) for CPDs or primary mouse monoclonal IgG_{2b} anti-8-hydroxy-guanosine antibody (Santa Cruz Biotechnologies, Dallas, TX, USA) for 8-OHdG at 2.5 µg/mL or an equivalent concentration of isotype control, followed by three TBS-T washes. The cells were incubated with biotinylated goat anti-mouse IgG secondary antibody (ThermoFisher Scientific, Waltham, MA, USA) diluted to 1:500 in Tris-buffered saline with 0.1% Tween 20 (TBS-T) for 15 min followed by three TBS-T washes. Horseradish peroxidase (HRP)-Streptavidin Conjugate (Invitrogen, Waltham, MA, USA) diluted 1:150 in TBS-T was added for 15 min followed by three TBS-T washes. The HRP substrate Diaminobenzidine (DAB) (Enhanced Liquid substrate System for Immunohistochemistry, Sigma-Aldrich, St. Louis, MO, USA) was added for 5 min followed by two MilliQ water washes. Isotype antibodies were run as controls for all experiments, but as previously published, the isotype controls resulted in minimal staining [83]. The coverslips were mounted on glass slides with entellen rapid mounting medium (Merck, Darmstadt, Germany) for image analysis [55].

- Skin explants:

After 3 h incubation, skin samples were fixed in 10% (*v*/*v*) neutral buffered formalin overnight, then paraffin-embedded and sectioned. The paraffin-embedded sections were first deparaffinized in xylene (ThermoFisher Scientific, Waltham, MA, USA), then hydrated by passing the slides through graded alcohol. Antigen retrieval was carried out by treating sections with citrate buffer, pH 6, at 95 °C for 30 min as previously described [56].

CPDs or 8-OHdG: Only for 8-OHdG staining, sections were incubated with RNase A (AMRESCO, Cleveland, OH, USA) at 37 °C for 30 min to remove 8-OHdG that would otherwise be detected in cellular RNA [84], followed by two TBS-T washes. For both lesions, sections were treated with 2 N HCl (Sigma-Aldrich, St. Louis, MO, USA) in 70% ethanol for 15 min at room temperature to denature DNA and further expose damaged sites. Following aspiration, the residual acid solution was neutralized with 50 mM Tris-HCl (pH 7.5) for 15 min at room temperature, followed by two further TBS-T washes. Sections were then blocked with 10% (*v*/*v*) horse serum in PBS, pH 7.2, for 60 min at room temperature, then incubated with primary antibody for 60 min at room temperature, either mouse monoclonal anti-thymine dimer at 10 µg/mL for CPDs or primary mouse monoclonal IgG_{2b} anti-8-hydroxy-guanosine antibody at 2.5 µg/mL for 8-OHdG or an equivalent concentration of isotype control, followed by three TBS-T washes.

XPC or *XPA*: Following the antigen retrieval, the XPC and XPA sections were blocked with avidin and biotin from the Dako Cytomation Blocking System (Dako, Glostrup, Denmark) for 10 min at room temperature with a brief rinse in between treatments, followed by blocking with 10% (*v*/*v*) horse serum in PBS for 60 min at room temperature. The sections were incubated with primary antibodies overnight at 4 °C, either with mouse monoclonal IgG_{2a} XPC at 2.5 µg/mL, mouse monoclonal IgG_1 XPA antibody at 4.0 µg/mL (both from Santa Cruz Biotechnology, Dallas, TX, USA), or an equivalent concentration of isotype control, followed by three TBS-T washes.

Detection of antibody binding: This was carried out for all sections with the Dako LSAB Plus REAL Detection System Kit with AEC chromogen staining, using the methods provided by the manufacturer (Dako, Glostrup, Denmark). The slides were mounted with DPX (Sigma-Aldrich, St. Louis, MO, USA) and coverslipped.

2.5. Image Acquisition

- Keratinocytes: Bright-field images were acquired on the Olympus stereo investigator scope (MBF Bioscience, Williston, VT, USA) or on the Zeiss AxioScan-Z1 slide scanner (Zeiss Microscopy, Oberkochen, Germany) at the Bosch Advanced Microscopy Facility (University of Sydney). All images were taken at 20× magnification, and the immunohistochemical images were analyzed using ImageJ software. Using this program, images from an individual experiment were thresholded to the same value. The regions of interest (ROI) were randomly selected. The means and standard errors of the mean (SEMs) from three to five ROI per coverslip of each treatment were calculated and graphed. Staining and image analysis for CPDs and 8-OHdG produced similar results to those obtained using endonuclease detection of the lesion, followed by Comet assay [54,76].
- Skin explants: Bright-field images were captured using the Zeiss Axio Scan (Zeiss Microscopy, Oberkochen, Germany). For each section, images of the whole skin section were taken at 20× magnification. All images were analyzed using MetaMorph imaging software (Molecular Devices Corporation, San Jose, CA, USA), whereby the epidermal area was isolated and thresholded specific for positive nuclei in this region. This software then automatically calculated the positive nuclei as a percentage of the total epidermal area.

2.6. siRNA Transfection

Plated keratinocytes were transfected with 50 nM siRNA directed at XPC (siXPC), XPA (siXPA), or a control non-directed sequence (siCTRL) (all from Santa Cruz Biotechnologies, Dallas, TX, USA), following combination with a lipid-based transfection reagent (Santa Cruz Biotechnologies, USA) in Opti-MEM™ serum-free media (ThermoFisher Scientific, MA, USA) according to the manufacturer's instructions and as previously described [85]. The cells were incubated overnight, and on the following day, an equal volume of 10% (*v*/*v*) FCS in KGM without EGF and cholera toxin was added to deliver a final concentration of 5% (*v*/*v*) KGM without EGF and cholera toxin. The cells were further incubated overnight under standard culture conditions prior to irradiation and treatment.

2.7. Western Blot

Keratinocytes were plated directly in six-well plates in KGM with supplements. Following the indicated treatments, the cells were lysed and subjected to Western blot as previously described [79] with minor modifications. The transfer of protein to a nitrocellulose membrane (AmershamTM Protran 0.45 lm NC; GE Healthcare) was achieved at 25 V overnight at 4 °C. The membrane was then blocked with 5% (*w*/*v*) BSA in TBS-T at pH 7.2 for 1 h before being incubated with mouse monoclonal IgG_{2a} XPC (Santa Cruz Biotechnologies, CA, USA) at 1 µg/mL in 5% (*w*/*v*) BSA in TBS-T, overnight at 4 °C. The following day, the membrane was washed with TBS-T three times and incubated with secondary goat anti-mouse IgG HRP-linked antibody (Cell Signaling Technology, Danvers,

MA, USA) in 5% (*w*/*v*) BSA in TBS-T for 1 h at room temperature. After incubation, the membrane was washed three times with TBS-T before adding chemiluminescence substrate (Millipore SAS, Molsheim, France) for band detection. The bands were imaged with the ChemiDocTM imaging system (Bio-Rad Laboratories, Inc., Hercules, CA, USA) at the Bosch Research Institute (University of Sydney), and densitometry was carried out using ImageJ software (version 1.50).

2.8. Unscheduled DNA Synthesis

This was carried out as previously described [79]. In brief, EDU (5-ethynyl-2′-deoxyuri dine) incorporation into nuclear DNA was detected using the iClick^{TM} EdU Andy Fluro 488 Imaging Kit (GeneCopoeia Inc, Rockville, MD, USA). The incorporation of this thymidine analog in a punctate pattern, in keratinocytes cultured without growth factors EGF and cholera toxin, measured unscheduled DNA synthesis rather than DNA replication [86]. Densitometry was performed using ImageJ software. The stained cells were manually counted from the images taken with a Zeiss LSM 510 Meta confocal microscope (Zeiss Microscopy, Oberkochen, Germany). The fluorescence intensity was measured in cells that were above the detection threshold and considered "UDS positive", and fluorescence images were acquired by confocal microscopy and analyzed using ImageJ software [79].

2.9. Seahorse Energetics

An XF96 Extracellular Flux Analyzer (Seahorse Bioscience, Agilent, CA, USA) at Bosch Research Institute, University of Sydney, was used immediately following irradiation of cells to measure ECAR, as previously described [79].

2.10. ATP Measurement

ATP levels were determined using the CellTiter-Glo® 2.0 Assay (Promega Corporation, Madison, WI, USA) as previously described [79].

2.11. ROS Measurement

ROS levels were measured using the ROS-Glo™ H2O2 assay (Promega Corporation, WI, USA) as previously described [79].

2.12. Statistical Analysis

- In vitro: Three independent experiments with triplicates per each treatment group were performed for each study with similar results, using keratinocytes from different donors. Unless otherwise indicated, the analyses were carried out by ANOVA with Tukey multiple comparisons post-test (GraphPad Prism statistical program) (CA, USA).
- Ex vivo: Three independent experiments were performed for each study with skin from different donors with similar results. Comparisons between treatments were made by one-way ANOVA followed by Sidak's multiple comparisons test, using the GraphPad Prism statistical program (CA, USA), unless otherwise stated. The data in the graphs represent the mean + SEM, unless otherwise stated.

3. Results

3.1. 24(OH)L_3 Reduced UV-Induced CPDs and 8-OHdG in a Concentration-Dependent Manner, Similar to 1,25(OH)$_2$$D_3$ in Human Primary Keratinocytes

UV-induced CPDs and 8-OHdG were increased in UV-irradiated vehicle-treated cells compared with non-UV-irradiated cells (Figure 2A,B; $p < 0.0001$, $p < 0.001$). In UV-irradiated keratinocytes, treatment with either 24(OH)L_3 or 1,25(OH)$_2$$D_3$ significantly reduced UV-induced CPDs ($p < 0.01$) (Figure 2A) and 8-OHdG ($p < 0.05$) (Figure 2B) at 1×10^{-10} M and higher concentrations ($p < 0.001$).

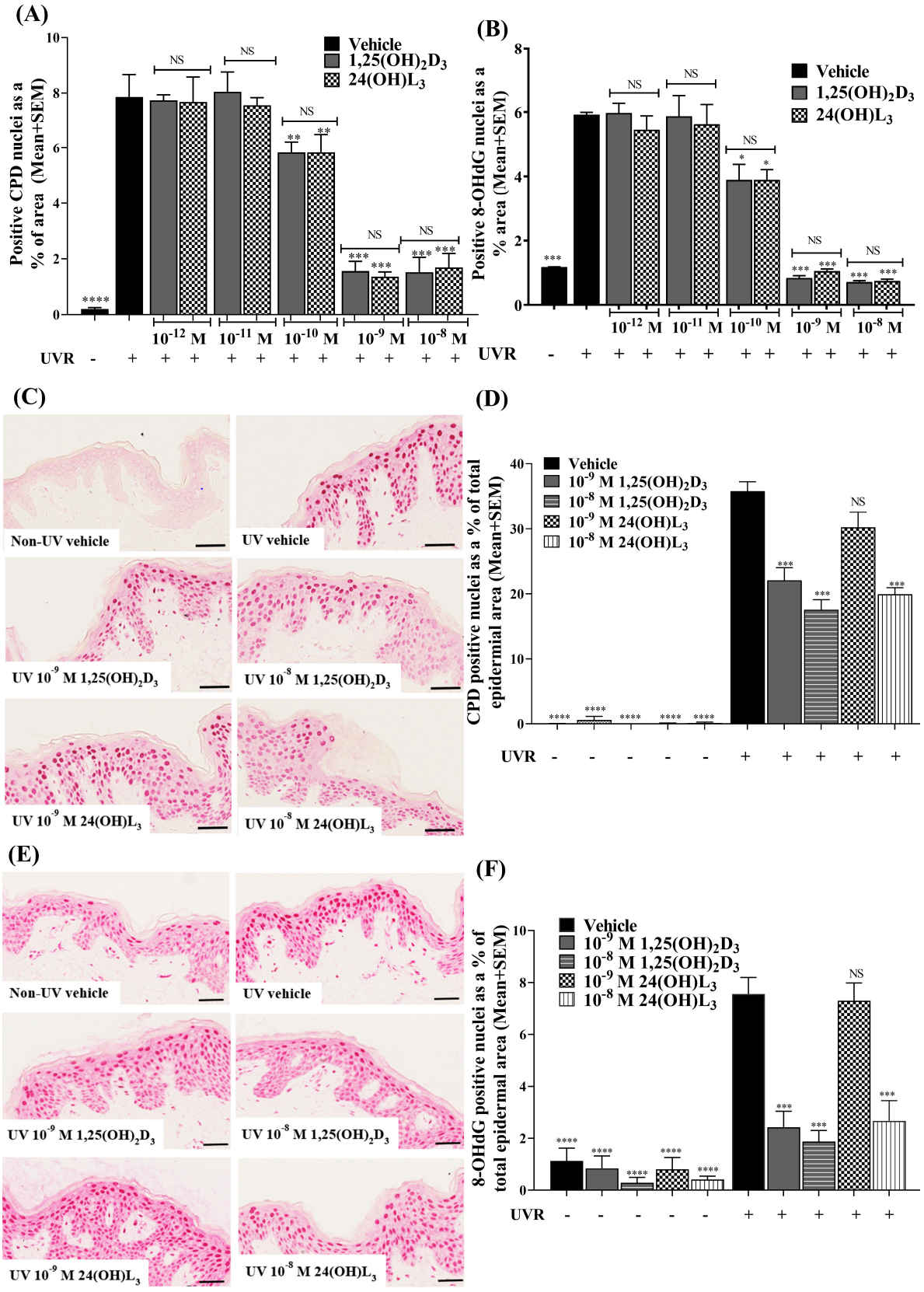


Figure 2. Concentration-dependent reduction of UV-induced CPDs or 8-OHdG by 1,25(OH)$_2$D$_3$ or 24(OH)L$_3$ in human primary keratinocytes and human skin explants. Human keratinocytes or skin

explants were exposed to solar simulated UV and then treated immediately after with vehicle, 0.1% (*v*/*v*) ethanol, or the positive control, 1,25(OH)$_2$D$_3$, or 24(OH)L$_3$ at five different concentrations (keratinocytes) or 1×10^{-9} M or 1×10^{-8} M (skin explants) for 3 h after irradiation, followed by immunohistochemical staining for CPDs (**A**,**C**,**D**) or 8-OHdG (**B**,**E**,**F**) photolesions. Densitometry of keratinocytes is presented as (**A**) CPD-positive nuclei as a % area and (**B**) 8-OHdG-positive nuclei as a % area. Results for keratinocytes are presented as mean + SEM from a single experiment performed in triplicate, representative of three separate experiments with similar results. Representative photomicrographs of immunohistochemical staining of UV-induced (**C**) CPDs and (**D**) 8-OHdG (scale bar = 50 µm). Metamorph analysis of IHC images of skin explants presented as (**E**) CPD- and (**F**) 8-OHdG-positive nuclei as percentage of total epidermal area. Results are from a single experiment performed with five explants per group. Presented as mean + SEM; * $p < 0.05$, ** $p < 0.01$, *** $p < 0.001$, **** $p < 0.0001$, when compared with UV vehicle; NS—not significant between datasets.

3.2. 24(OH)L$_3$ Reduced UV-Induced CPDs and 8-OHdG at Higher Concentrations Than 1,25(OH)$_2$D$_3$ in Human Skin Explants

Very low levels of CPDs (Figure 2C,D) and 8-OHdG (Figure 2E,F) were observed in non-UV-exposed skin explants compared with UV-irradiated vehicle-treated human skin explants ($p < 0.0001$). For the skin explants treated immediately after UV irradiation with either 1×10^{-9} M or 1×10^{-8} M 1,25(OH)$_2$D$_3$, there were significant reductions in UV-induced CPDs (Figure 2C,D; $p < 0.001$) and 8-OHdG (Figure 2E,F; $p < 0.001$). Treatment with 1×10^{-8} M 24(OH)L$_3$ also significantly reduced both CPDs and 8-OHdG ($p < 0.001$ for both), but no significant reductions in either type of DNA damage were observed after treatment with 1×10^{-9} M 24(OH)L$_3$ (Figure 2C–F).

3.3. 24(OH)L$_3$ Increased Unscheduled DNA Synthesis Similar to 1,25(OH)$_2$D$_3$ in UV-Irradiated Human Primary Keratinocytes

To examine whether these vitamin-D-related compounds increased DNA repair, we tested unscheduled DNA synthesis (UDS). UV-irradiated keratinocytes or non-irradiated control cells were treated immediately after with vehicle, 1,25(OH)$_2$D$_3$ or 24(OH)L$_3$ in the presence of 5-ethynyl-20-deoxyuridine (EDU) for 1.5 h. UDS-positive nuclei, a measure of DNA repair under the circumstances of the experiment where the keratinocytes were quiescent [86], were detected as punctate nuclei with fluorescent staining (Figure 3A–C). The UDS incidence was assessed as the percentage of UDS-positive cells in 1000 randomly selected cells. While there was a low incidence of UDS positivity in non-irradiated cells treated with vehicle, 1,25(OH)$_2$D$_3$ or 24(OH)L$_3$ (Figure 3A,D), UV-irradiated 1,25(OH)$_2$D$_3$- ($p < 0.001$) or 24(OH)L$_3$-treated cells ($p < 0.0001$) showed a significantly higher UDS incidence than the UV vehicle-treated cells (Figure 3A,D). UDS was also quantified as the average intensity of the positive fluorescence of nuclei (Figure 3C,E), where low, not significant intensity was observed in UV vehicle-treated cells and non-UV cells. The UV-irradiated cells treated with either 1,25(OH)$_2$D$_3$ ($p < 0.0001$) or 24(OH)L$_3$ ($p < 0.0001$) have significantly increased intensity of EDU incorporation compared with UV-irradiated vehicle-treated cells (Figure 3C,E).

3.4. 24(OH)L$_3$ Increased ATP Levels Similar to 1,25(OH)$_2$D$_3$ in UV-Irradiated Human Primary Keratinocytes

DNA repair requires energy [38,87]. Exposure to UV irradiation reduced ATP levels in keratinocytes (Figure 3F). Treatment with 24(OH)L$_3$ or 1,25(OH)$_2$D$_3$ immediately after UV increased the ATP levels measured 1.5 h after UV exposure in keratinocytes ($p < 0.05$) compared with the UV vehicle. Significant differences were not observed between the different concentrations of either 24(OH)L$_3$ or 1,25(OH)$_2$D$_3$. Significant changes in ATP levels were not observed in non-irradiated cells treated with either 24(OH)L$_3$ or 1,25(OH)$_2$D$_3$ compared with the non-UV vehicle (Figure 3F).

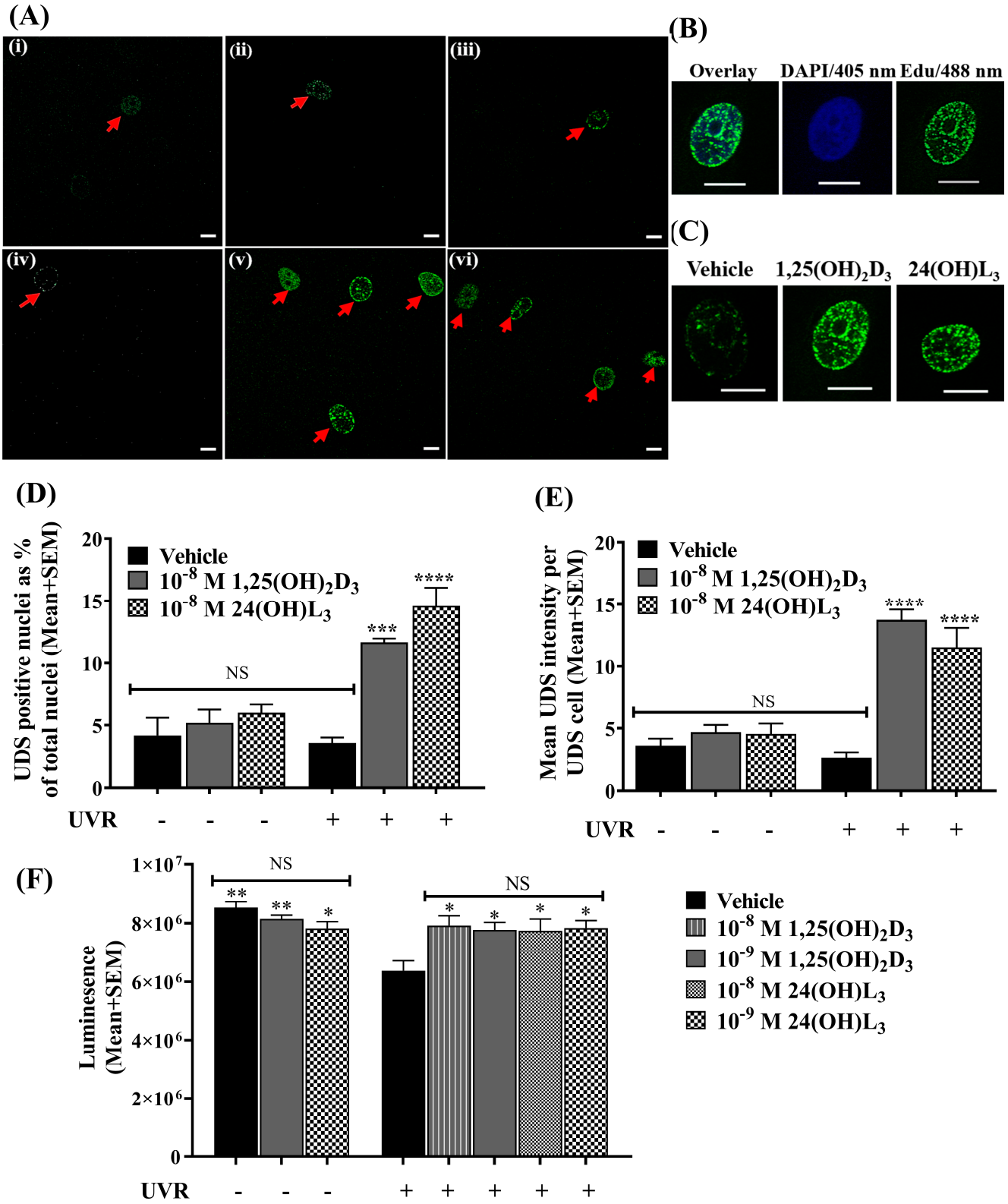


Figure 3. Unscheduled DNA synthesis (UDS) and ATP levels increased in human primary keratinocytes after UV exposure and treatment with $1,25(OH)_2D_3$ or $24(OH)L_3$ following UV irradiation. (**A**) Example confocal images for incidence of UDS-positive nuclei: (**i**) non-UV vehicle, 0.1% (*v*/*v*) ethanol; (**ii**) non-UV $1,25(OH)_2D_3$ (1×10^{-8} M); (**iii**) non-UV $24(OH)L_3$ (1×10^{-8} M); (**iv**) UV vehicle,

0.1% (*v*/*v*) ethanol; (**v**) UV 1,25(OH)$_2$D$_3$ (1×10^{-8} M); and (**vi**) UV 24(OH)L$_3$ (1×10^{-8} M) (scale = 10 μm). (**B**) Example confocal images of UDS-positive nuclei showing EDU incorporation with DAPI counterstain (EDU incorporation shown by punctate nuclei) (scale = 10 μm). (**C**) Example confocal images of EDU intensity in UV-irradiated cells treated with vehicle, 1,25(OH)$_2$D$_3$, or 24(OH)L$_3$. (**D**) UDS-positive nuclei as a percentage of total nuclei, for randomly counted 1000 nuclei per treatment group, 1.5 h after UV irradiation. (**E**) Average EDU intensity per UDS-positive cell nuclei (15 nuclei for each treatment). (**F**) ATP levels measured by CellTiterGlo 2.0 assay at 1.5 h after UV exposure and treatments. Results were from a single experiment performed in triplicate, representative of two separate experiments with similar results, presented as mean + SEM; * $p < 0.05$, ** $p < 0.01$, *** $p < 0.001$, **** $p < 0.0001$, compared with UV vehicle; NS—not significant between datasets.

3.5. 24(OH)L$_3$ Increased Glycolysis Similar to 1,25(OH)$_2$D$_3$ in UV-Irradiated Human Primary Keratinocytes

We previously reported that the oxygen consumption rate (a measure of oxidative phosphorylation) decreased in UV-exposed keratinocytes [79]. Thus, in order to determine the source of the energy in these irradiated and treated keratinocytes, the extracellular acidification rate (ECAR), a measure of glycolysis, was measured using Seahorse XF analysis (Figure 4A). The results indicated that there were no significant changes in the non-irradiated or irradiated keratinocytes over the first 25 min of equilibration after sham or UV exposure prior to the injection of treatments. Significant increases in the ECAR, indicating increased glycolysis, were observed in UV-irradiated, 24(OH)L$_3$-treated cells ($p < 0.01$) and in UV-irradiated, 1,25(OH)$_2$D$_3$-treated cells ($p < 0.05$) (Figure 4B) compared with UV-irradiated vehicle-treated keratinocytes.

The ATP synthase inhibitor, oligomycin, an inhibitor of oxidative phosphorylation, reduced ATP production due to disruption in the electron transport chain [88,89]. The injection of oligomycin significantly increased ECAR in non-UV-exposed vehicle- ($p < 0.001$), 1,25(OH)$_2$D$_3$- ($p < 0.0001$), and 24(OH)L$_3$-treated keratinocytes ($p < 0.01$). This was due to a switch from oxidative phosphorylation to glycolysis and was previously observed in these cells [79]. As seen in Figure 4A,C, the ECAR was unchanged after oligomycin treatment in UV-irradiated cells, consistent with the proposal that oxidative phosphorylation was impaired in these cells after UV. The analogue 2-deoxy-D-glucose (2DG) is a glucose analogue that competitively inhibits glucose uptake and competitively inhibits hexokinase and thus glycolysis [90]. The analogue 2DG significantly reduced the oligomycin-induced glycolysis in non-irradiated cells ($p < 0.0001$), as well as in UV-irradiated vehicle- ($p < 0.01$), 1,25(OH)$_2$D$_3$- ($p < 0.001$), and 24(OH)L$_3$-treated ($p < 0.001$) cells (Figure 4D).

3.6. Reductions in UV-Induced CPDs and 8-OHdG by 24(OH)L$_3$ or 1,25(OH)$_2$D$_3$ Were Abolished in the Presence of the Glycolysis Inhibitor (2-Deoxy-D-glucose) but Not by the Oxidative Phosphorylation Inhibitor (Oligomycin) in Human Primary Keratinocytes

If increased glycolysis was the source of the energy to increase DNA repair and thus reduce DNA damage in UV-irradiated keratinocytes, then the inclusion of 2-deoxy-D-glucose (2DG) should impair DNA damage reduction, while the addition of oligomycin should have no effect. As previously observed, the addition of 24(OH)L$_3$ or 1,25(OH)$_2$D$_3$ significantly reduced the CPDs (Figure 5A,B) and 8-OHdG (Figure 5C,D) in human primary keratinocytes after UV ($p < 0.001$). Treatment with 2DG abolished the reduction of UV-induced CPDs and 8-OHdG by 24(OH)L$_3$ or 1,25(OH)$_2$D$_3$ measured 1.5 h after irradiation. Treatment with oligomycin did not affect the reduction of UV-induced CPDs or 8-OHdG with 24(OH)L$_3$ or 1,25(OH)$_2$D$_3$ after 1.5 h. Treatment with the combination of 2DG and oligomycin also abolished the reduction of UV-induced photolesions in the presence of 24(OH)L$_3$ and 1,25(OH)$_2$D$_3$ to a similar extent as 2DG alone (Figure 5A–D).

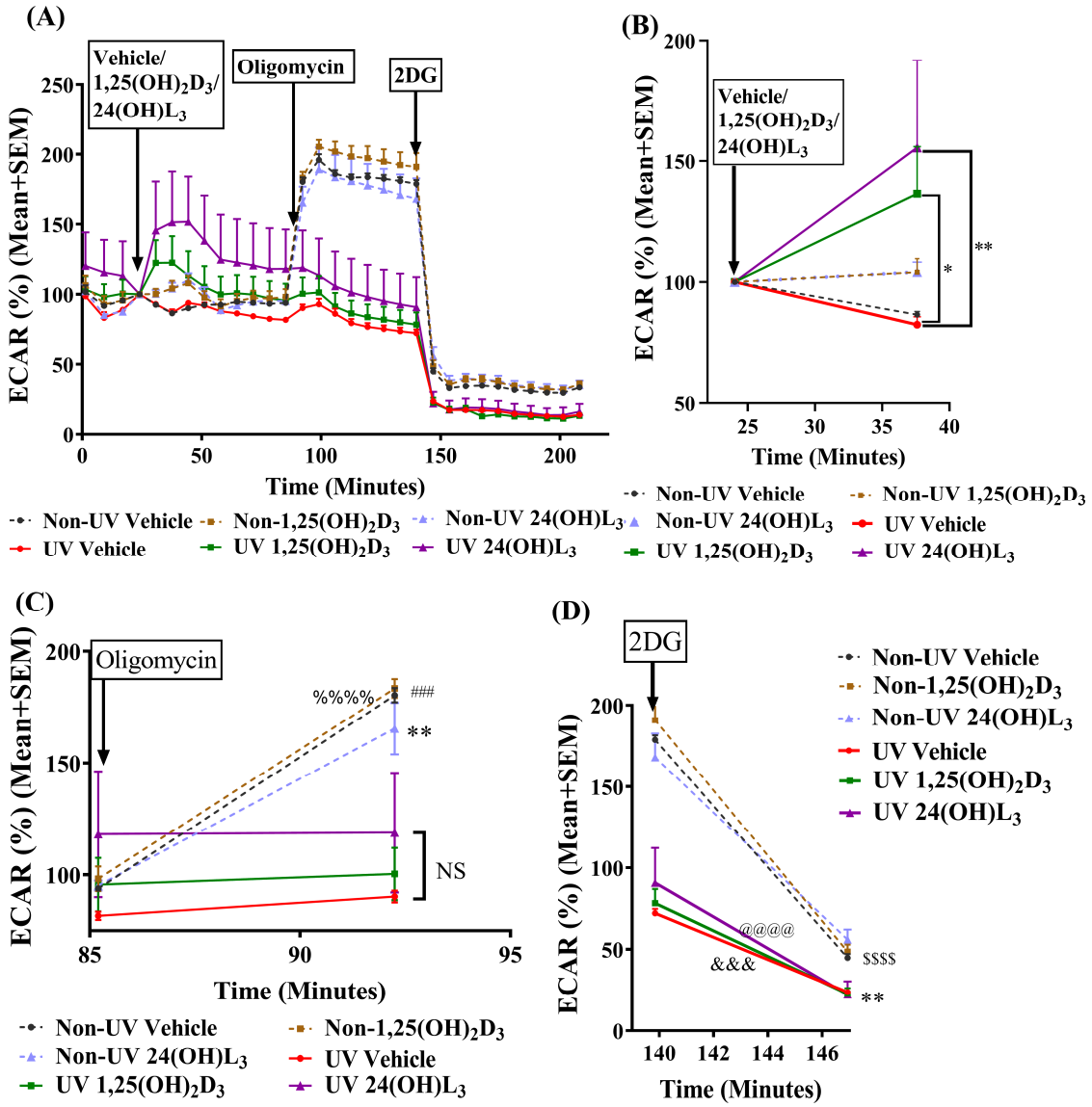


Figure 4. The extracellular acidification rate (ECAR) was increased by treatment with 24(OH)L_3 or 1,25(OH)$_2$D$_3$, in UV-irradiated human primary keratinocytes. (**A**) Keratinocytes were subjected to Seahorse XF analysis after UV exposure (UV) or non-UV, and treatments were added at the point of injections, indicated by arrows. Data were normalized using the Seahorse XF Normalization System. (**B**) ECAR following injection of vehicle, 0.1% (*v*/*v*) ethanol, 1×10^{-8} M 1,25(OH)$_2$D$_3$, or 1×10^{-8} M 24(OH)L_3, 25 min after injection (n = 14). The ECAR significantly increased in UV 24(OH)L_3 cells (** $p < 0.01$) and in UV 1,25(OH)$_2$D$_3$ cells (* $p < 0.05$) compared with the UV vehicle. (**C**) ECAR following 10 µM oligomycin injection. Significantly different from the point of oligomycin injection in the non-UV vehicle ($^{\#\#\#}$ $p < 0.001$), non-UV-1,25(OH)$_2$D$_3$ ($^{\%\%\%\%}$ $p < 0.0001$), or non-UV-24(OH)L_3 (** $p < 0.01$), NS, between UV-irradiated cells. (**D**) ECAR after 50 mM 2-deoxy-D-glucose (2-DG) injection. Significantly different from the point of injection, non-UV vehicle, non-UV 1,25(OH)$_2$D$_3$, non-UV 24(OH)L_3 ($^{\$\$\$\$}$ $p < 0.0001$), UV vehicle (** $p < 0.01$), UV 1,25(OH)$_2$D$_3$ ($^{\&\&\&}$ $p < 0.001$), and UV 24(OH)L_3 ($^{@@@@}$ $p < 0.0001$). Results are presented as mean + SEM, compared with the UV vehicle. NS—not significant between datasets.

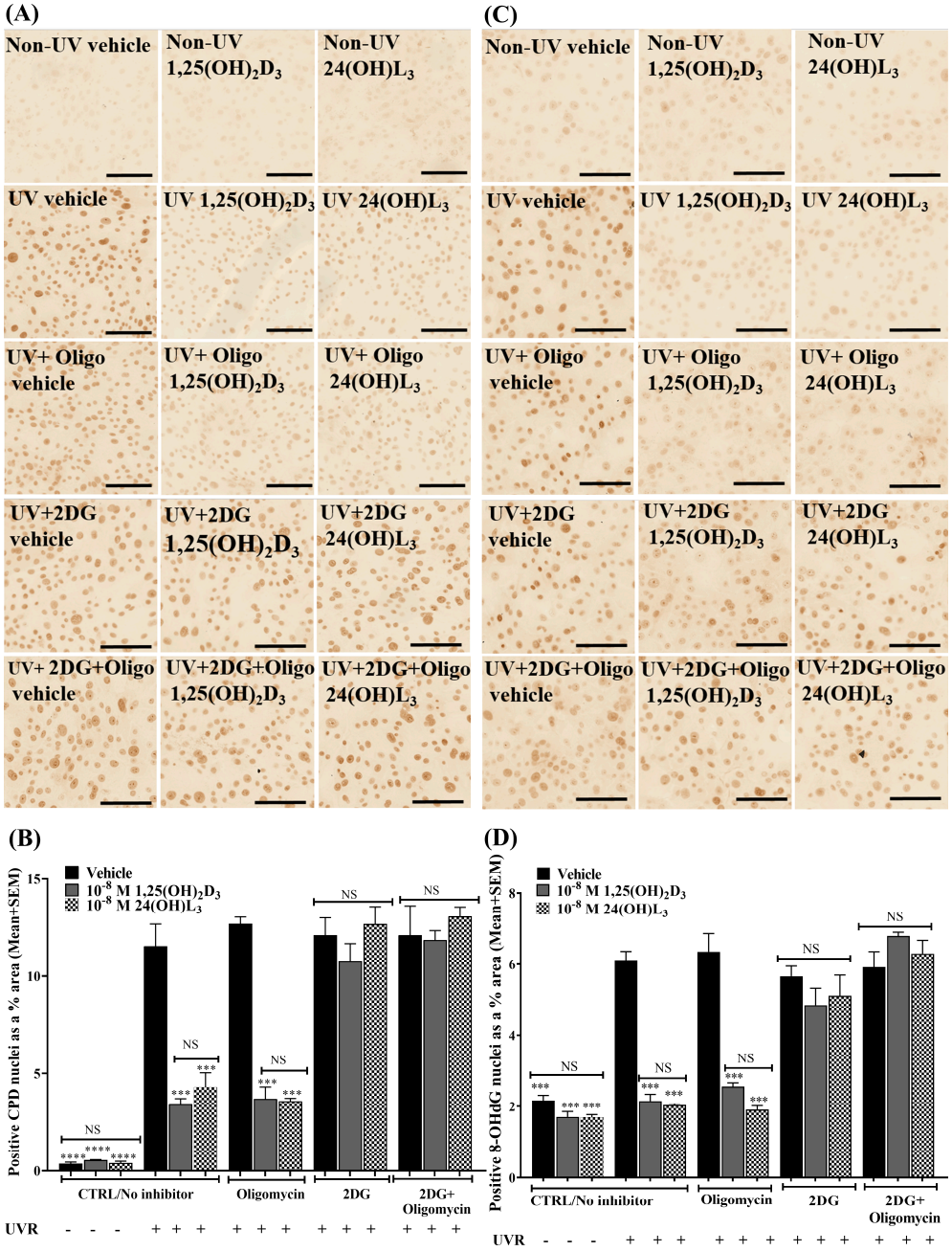


Figure 5. UV-induced CPDs and 8-OHdG reduction by 24(OH)L_3 or 1,25(OH)$_2$$D_3$ was abolished by 2-deoxy-D-glucose (2DG) but not by oligomycin in human primary keratinocytes. (**A**) Example bright-field confocal IHC photomicrographs of UV-induced CPDs in keratinocytes treated with vehicle, 0.1% (v/v) ethanol, 1×10^{-8} M 1,25(OH)$_2$$D_3$, or 1×10^{-8} M 24(OH)L_3 for 1.5 h in the presence or absence of 50 mM 2DG, 10 μM oligomycin, or a combination of 50 mM 2DG and 10 μM oligomycin (scale bar = 100 μm). (**B**) Densitometry presented as CPD-positive nuclei as a % area, 1.5 h after UV irradiation. (**C**) Example bright-field confocal IHC photomicrographs of UV-induced 8-OHdG treated with vehicle, 0.1% (v/v) ethanol, 1×10^{-8} M 1,25(OH)$_2$$D_3$, or 1×10^{-8} M 24(OH)L_3 for 1.5 h in the presence or absence of 50 mM 2DG, 10 μM oligomycin, or a combination of 50 mM 2DG and 10 μM oligomycin (scale bar = 100 μm). (**D**) Densitometry presented as 8-OHdG-positive nuclei as a % area, 1.5 h after UV irradiation. Mean + SEM; **** $p < 0.0001$ *** $p < 0.001$, when compared with UV vehicle; NS—not significant between datasets.

3.7. 24(OH)L_3 Reduced Reactive Oxygen Species (ROS) Similar to 1,25(OH)$_2$$D_3$ in UV-Irradiated Human Primary Keratinocytes

The generation of ROS by UV exposure directly causes oxidative DNA damage [91] and inhibits DNA repair [34]. As expected, UV irradiation increased the ROS levels in keratinocytes (Figure 6A,B). Treatment with either 24(OH)L_3 or 1,25(OH)$_2$$D_3$ immediately after irradiation significantly reduced ROS levels in keratinocytes ($p < 0.0001$) compared with the UV vehicle, when measured either 15 min after UV (Figure 6A) or 1.5 h after UV for 24(OH)L_3 ($p < 0.01$) and for 1,25(OH)$_2$$D_3$ ($p < 0.05$) (Figure 6B).

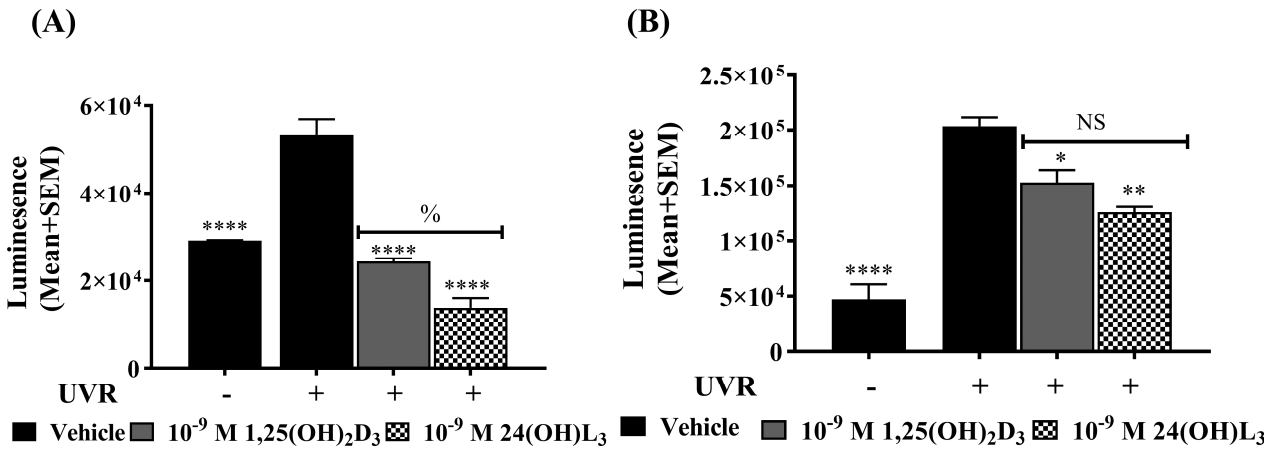


Figure 6. Reactive oxygen species (ROS) were reduced in UV-irradiated human keratinocytes treated with either 24(OH)L_3 or 1,25(OH)$_2$$D_3$. (**A**) Human primary keratinocytes were irradiated and immediately treated with either vehicle, 0.1% (*v*/*v*) ethanol, 1×10^{-9} M 1,25(OH)$_2$$D_3$, or 1×10^{-9} 24(OH)L_3, and ROS levels were measured using the ROS-Glo™ commercial assay after (**A**) 15 min or (**B**) 90 min after irradiation. Results were from a single experiment performed in triplicate, representative of two separate experiments with similar results. Mean + SEM; **** $p < 0.0001$, ** $p < 0.01$, * $p < 0.05$ when compared with UV vehicle, $^{\%}$ $p < 0.05$ for UV-1,25(OH)$_2$$D_3$ vs UV-24(OH)L_3 after 15 min; NS—not significant between datasets.

3.8. Topical Treatment with 1,25(OH)$_2$$D_3$ or 24(OH)L_3 Increased XPC and XPA in UV-Irradiated Skin Explants

If CPD repair by the nucleotide excision repair (NER) pathway were increased, it would be expected that an increase in key NER proteins such as XPC and XPA would be observed. In UV-irradiated, vehicle-treated skin explants, there was a small but not significant increase in XPC (Figure 7A,B) or XPA (Figure 7C,D), compared with non-irradiated skin explants. In contrast, significant increases in XPC ($p < 0.01$) (Figure 7B) and XPA ($p < 0.01$) (Figure 7D) were observed in skin explants treated topically with 1×10^{-9} M 1,25(OH)$_2$$D_3$. Treatment with 1×10^{-8} M 24(OH)L_3 significantly increased both XPC and XPA ($p < 0.05$), but there was no significant increase in either protein after treatment with 1×10^{-9} M 24(OH)L_3 (Figure 7B,D).

3.9. Reductions of UV-Induced CPDs by 1,25(OH)$_2$$D_3$ and 24(OH)L_3 Were Abolished by Knockdown of XPC or XPA

In order to see whether the NER proteins indeed were critical for the increased repair of CPDs, the keratinocytes were first transfected with small interfering RNA targeted to XPC mRNA (siXPC) or with a non-directed siRNA sequence (siCTRL), as described in [92]. XPC knockdown by siRNA was verified by Western blot (Figure 8A). Human primary keratinocytes were irradiated 48 h after siRNA transfection and immediately treated with either vehicle or 1,25(OH)$_2$$D_3$ or 24(OH)L_3 each at 1×10^{-9} M for 3 h. Photomicrographs of immunohistochemical staining for UV-induced CPDs are presented in Figure 8B. The UV-irradiated vehicle-treated cells showed a significant increase in CPDs compared with non-

UV cells in cells transfected with a non-directed sequence (siCTRL) ($p < 0.0001$). Significant reductions in UV-induced CPDs were observed in cells treated with 1,25(OH)$_2$D$_3$ and 24(OH)L$_3$ ($p < 0.001$ for both) in the siCTRL samples. Reductions of CPDs with 1,25(OH)$_2$D$_3$ or 24(OH)L$_3$ were abolished in the presence of cells transfected with siRNA directed at XPC (siXPC) (Figure 8B,C).

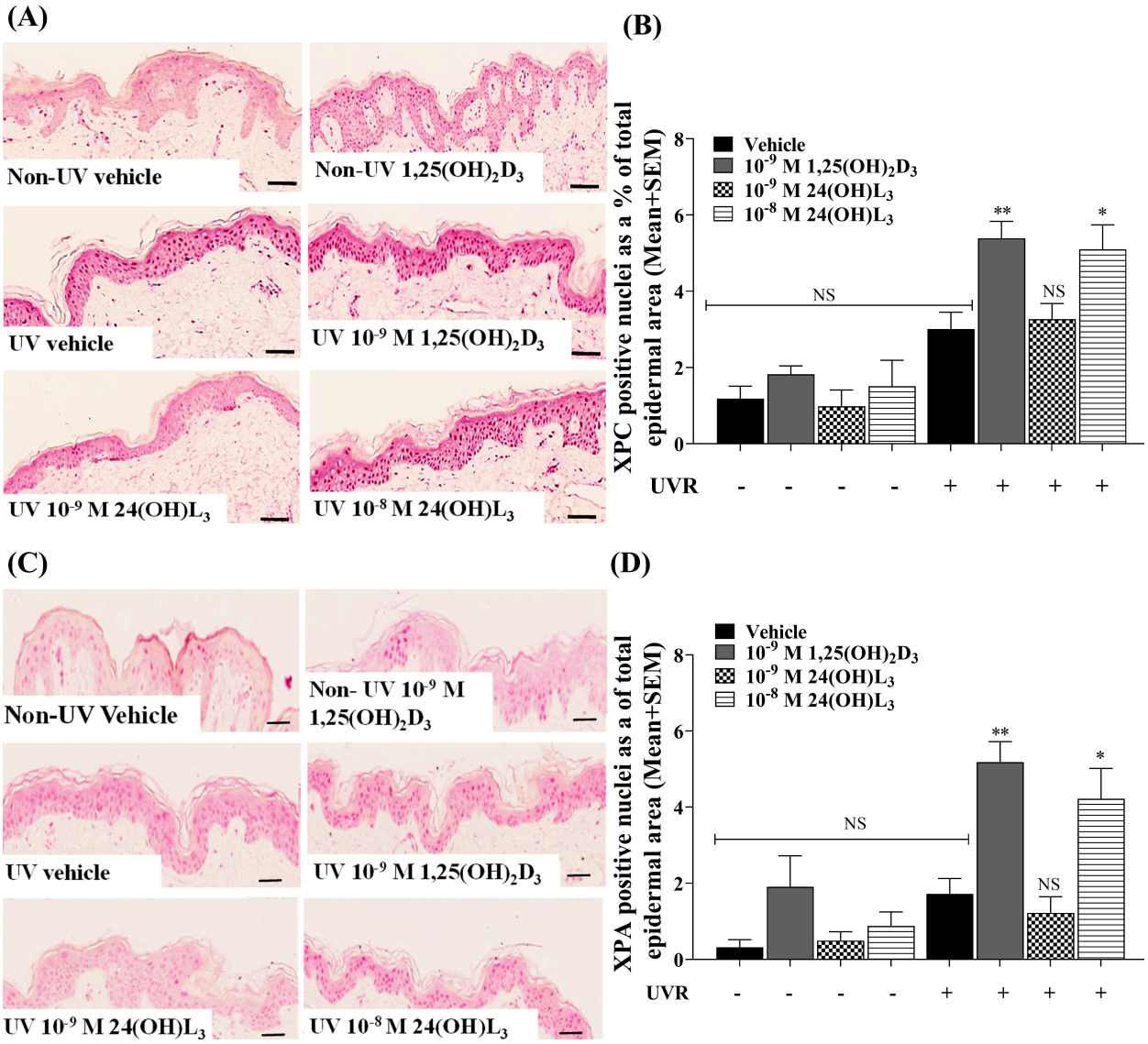


Figure 7. Topical treatment of human skin explants with 1,25(OH)$_2$D$_3$ or 24(OH)L$_3$ increased NER proteins XPC and XPA after UV. (**A**) Example bright-field confocal IHC photomicrographs of UV-induced XPC expression or (**C**) XPA expression in human skin explants, topically treated with vehicle, 0.1% (v/v) ethanol, 1×10^{-9} M 1,25(OH)$_2$D$_3$, 1×10^{-8} M, or 1×10^{-9} M 24(OH)L$_3$ for 3 h (scale bar = 50 μm). Densitometry presented as (**B**) XPC-positive nuclei as a % total epidermal area and (**D**) XPA-positive nuclei as a % total epidermal area. Results are from a single experiment performed using five skin explants per treatment, representative of three separate experiments with similar results. Mean + SEM; ** $p < 0.01$, * $p < 0.05$, when compared with UV vehicle; NS—not significant between datasets−.

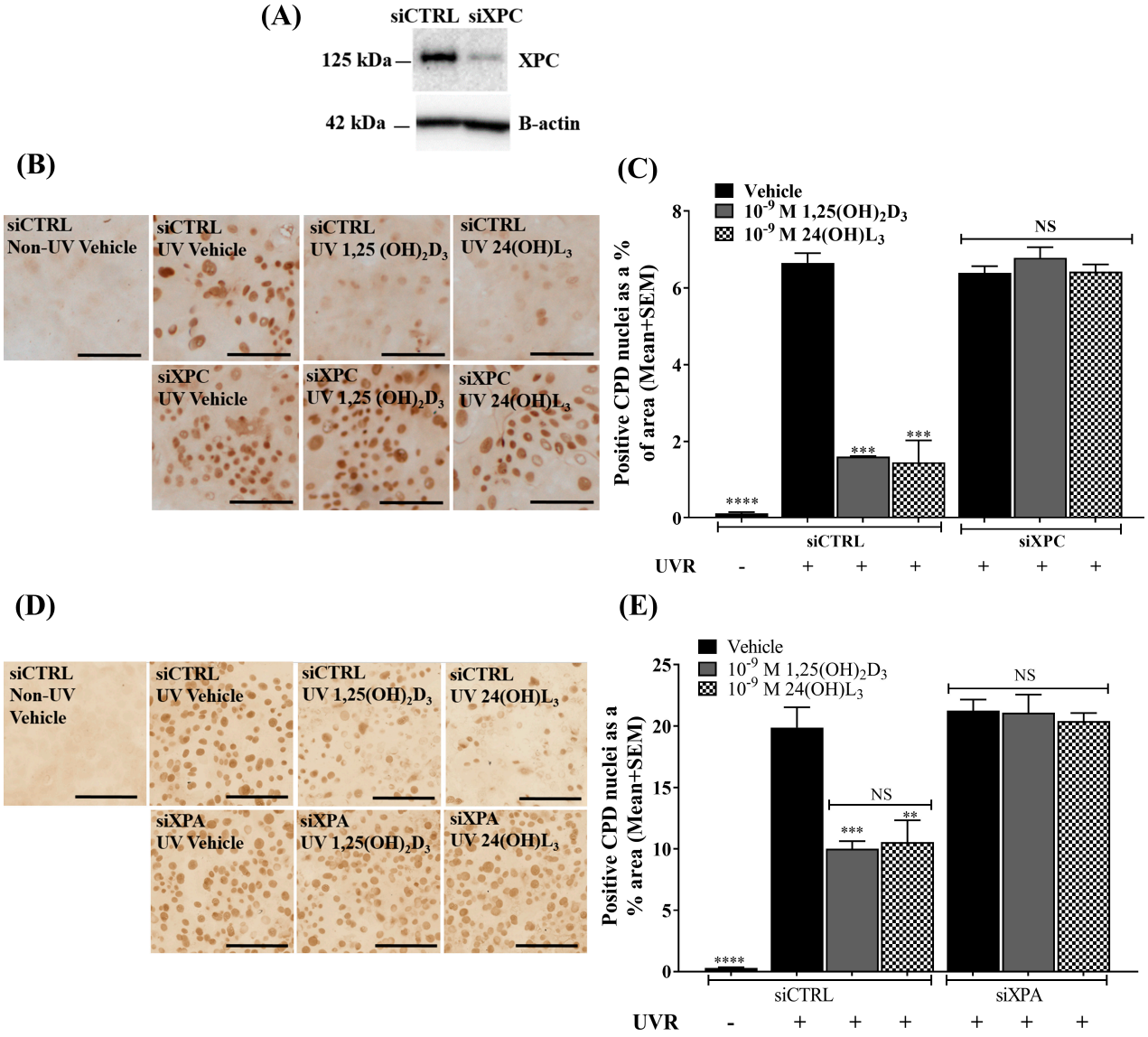


Figure 8. UV-induced CPD reduction by $1,25(OH)_2D_3$ or $24(OH)L_3$ was abolished by XPC or XPA knockdown in human primary keratinocytes. (**A**) Western blot showing the level of XPC protein in human primary keratinocytes following transfection with siCTRL or siXPC for 48 h. (**B**) Representative photomicrographs of IHC staining of UV-induced CPDs treated after UV with vehicle, 0.1% (*v*/*v*) ethanol, 1×10^{-9} M $1,25(OH)_2D_3$, or 1×10^{-9} M $24(OH)L_3$ after transfection with siCTRL or siXPC. Dark brown staining indicates the presence of CPD-positive nuclei (scale bar = 100 µm). (**C**) Image analysis of IHC images in panel B where values were calculated as CPD-positive nuclei as a % area. (**D**) Representative photomicrographs of immunohistochemical staining of UV-induced CPDs treated after UV with vehicle, 0.1% (*v*/*v*) ethanol, $1,25(OH)_2D_3$, or $24(OH)L_3$ after transfection with siCTRL or siXPA. Dark brown staining indicates the presence of CPD-positive nuclei (scale bar = 100 µm). (**E**) Image analysis of IHC images in panel D presented as CPD-positive nuclei as a % area. Results are from a single experiment performed in triplicate, representative of three separate experiments with similar results. Mean + SEM; **** $p < 0.0001$, *** $p < 0.001$, ** $p < 0.01$, when compared with UV siCTRL vehicle. NS—not significant between datasets.

A similar study was carried out in keratinocytes transfected with siRNA targeted to XPA mRNA (siXPA) or a non-directed siRNA sequence (siCTRL). Again, UV-irradiated vehicle-treated human primary keratinocytes showed significant increases in CPDs compared with non-irradiated cells in siCTRL samples (Figure 8D,E; $p < 0.0001$). UV-irradiated

keratinocytes treated with 1,25$(OH)_2D_3$ or 24(OH)L_3 for 3 h had significantly reduced UV-induced CPDs ($p < 0.001$ or $p < 0.01$ respectively) in siCTRL samples. The reduction of CPDs by 1,25$(OH)_2D_3$ or 24(OH)L_3 was abolished in cells transfected with siRNA directed at XPA (Figure 8D,E).

4. Discussion

The treatment with 1,25$(OH)_2D_3$ has been shown to reduce UV-induced DNA damage in skin in many studies [52,55,57,76,79,85,93–95]. The current study investigated the photoprotective properties of one of the most abundant "over-irradiation" metabolites, 24(OH)L_3, in comparison with 1,25$(OH)_2D_3$. This study tested only 24(OH)L_3. While further metabolism of 24(OH)L_3 by other CYP enzymes known to metabolize vitamin-D-related compounds is theoretically possible, there is no precedent for CYP24A1, which metabolizes 25-hydroxyvitamin D and 1,25$(OH)_2D_3$ to their 24-hydroxylated derivatives, to act on a sterol with an intact B-ring. Even though it is possible that CYP27A1 acts on 24(OH)L3, as it can act on other lumisterol compounds (R. Tuckey, personal communication), it is doubtful that there is enough CYP27A1 in skin to make a difference. Whether any metabolism of 24(OH)L3 by CYP27A1 changes biological activity is also unknown. UV-induced CPDs, as well as 8-OHdG, were reduced in a concentration-dependent manner by the addition of 24(OH)L_3 immediately after UV exposure, similar to 1,25$(OH)_2D_3$. In keratinocytes, both compounds were effective at a low concentration of 1×10^{-10} M, but in human skin explants, the minimal effective dose of 1,25$(OH)_2D_3$ to reduce both CPDs and 8-OHdG was 10-fold higher at 1×10^{-9} M. The minimal effective dose of 24(OH)L_3 in skin explants was a further 10-fold higher. It is likely that the thickness of epidermis in the human skin reduced the penetration of both compounds, with that of 24(OH)L_3 reduced to a greater extent than that of 1,25$(OH)_2D_3$, although this is yet to be investigated in more detail.

Our results indicated that at least part of the reason for the reduction in DNA damage with 24(OH)L_3 was an increase in DNA repair as evidenced by the increased intensity and number of UDS-positive nuclei in the presence of 24(OH)L_3 compared with the UV vehicle in UV-exposed keratinocytes. These increases were similar to those seen with 1,25$(OH)_2D_3$. As illustrated in Figure 3A,B, DNA repair was observed mainly in the nuclei of keratinocytes, although the repair of mitochondrial DNA cannot be entirely excluded. We have previously reported increased DNA repair after UV with 1,25$(OH)_2D_3$ [79]. DNA repair is an energy-intensive metabolic process. UV radiation damages mitochondria, and the damage impairs their main function, cellular respiration [31,96,97]. An earlier study by our group indicated that oxygen consumption rates, which are measures of oxidative phosphorylation, decreases after UV exposure [79]. As shown here, oligomycin, an inhibitor of oxidative phosphorylation [88,89], had no effect on the ECAR response of the UV exposed cells due to inactive oxidative phosphorylation. As expected, the treatment of the keratinocyte cultures with oligomycin also had no effect on the reduction of UV-induced DNA damage with 24(OH)L_3 or the hormonal form of vitamin D.

Although ATP levels were reduced after UV, treatment with either 1,25$(OH)_2D_3$ or 24(OH)L_3 increased ATP. We looked at an alternative source of energy, glycolysis. There were no significant changes in glycolysis, as measured by ECAR in UV-irradiated cells injected with vehicle. In contrast, glycolysis was increased by both 1,25$(OH)_2D_3$ and 24(OH)L_3 in UV-irradiated keratinocytes, as reported previously for 1,25$(OH)_2D_3$ [79]. Oligomycin increased ECAR in non-irradiated cells, indicating that oxidative phosphorylation was still intact in these cells, unlike the UV-exposed cells, as energy production in the cell switched from oxidative phosphorylation to glycolysis upon the addition of the oxidative phosphorylation inhibitor in the non-irradiated keratinocytes. As seen in Figure 4A, the addition of 2-deoxy-D-glucose suppressed glycolysis/ECAR in all keratinocytes. The addition of 2-deoxy-D-glucose to the keratinocytes also abolished the reduction in UV-induced CPDs and 8-OHdG by 1,25$(OH)_2D_3$ or 24(OH)L_3, consistent with the proposal that the active glycolysis produced by treatment with 1,25$(OH)_2D_3$ or 24(OH)L_3 was critical for the reduction in UV-induced DNA damage.

The electron transport chain in mitochondria is the main source of intrinsic ROS production in cells [98]. UV irradiation increases ROS production, and the damage to mitochondria by UV may further increase cellular ROS levels [99,100]. Increased ROS levels were observed in UV-irradiated keratinocytes at 15 min and 1.5 h post-UV. The UV-irradiated keratinocytes treated with $1,25(OH)_2D_3$ or $24(OH)L_3$ had significantly reduced ROS, indicating that these compounds could contribute to a reduction of ROS levels after UV. While one explanation could be just that $1,25(OH)_2D_3$ or $24(OH)L_3$ slowed oxidative phosphorylation, we have previously reported that the treatment of keratinocytes with $1,25(OH)_2D_3$ increased an early form of mitophagy [101], leading to mitochondrial repair [79] and reduced ROS. There are data indicating that $1,25(OH)_2D_3$ via the vitamin D receptor (VDR) is able to bind mitochondrial DNA and affect the transcription of oxidative phosphorylation subunits [102], while silencing of the VDR in various cell lines caused excessive ROS generation [103]. There is also evidence that $1,25(OH)_2D_3$ activates the Nrf2–Keap1 antioxidant pathway, which ameliorates oxidant stress [104–106], and that $1,25(OH)_2D_3$, lumisterol, and even tachysterol hydroxyderivatives do so in UV-exposed keratinocytes [107,108] and thus potentially reduce oxidative DNA damage. It is highly likely that reduced ROS levels as a result of treatment with $1,25(OH)_2D_3$ or $24(OH)L_3$ directly contribute to reduced 8-OHdG levels [91] and nitrosative stress [109] in UV-irradiated keratinocytes. Importantly, with reduced ROS and reactive nitrogen species [53,76], there will be less damage to cellular proteins, including proteins involved in DNA repair, and thus more effective repair [34,110]

Since the abovementioned mechanisms may collectively contribute to the increased DNA repair after UV, we explored two proteins involved in the nucleotide excision repair pathway for CPDs. XPC is an initial damage recognition protein in the GG–NER pathway, while XPA helps to verify the DNA damage and stabilize the DNA as it is repaired and is required for both GG–NER and TC–NER [111]. XPC and XPA accumulate at the sites of DNA damage [112]. UV-induced CPDs cause only a small distortion in the DNA helix and so are dependent for detection on the binding of XPE, a complex of damaged DNA binding proteins 1 and 2 (DDB1 and DDB2) [38]. DDB recruits XPC, which together with XPA is required for the successful initiation of NER [113]. In the current study, the XPC and XPA protein levels were increased in response to treatment with the lumisterol-derived $24(OH)L_3$ as well as $1,25(OH)_2D_3$ in UV-irradiated human explants. Furthermore, knockdown of either XPC or XPA abolished the reduction in CPDs normally seen after the addition of either $1,25(OH)_2D_3$ or $24(OH)L_3$, indicating key roles for these proteins in this process. No other changes in DNA repair proteins after $1,25(OH)_2D_3$ or $24(OH)L_3$ treatment were examined in this study. It has previously been reported that the treatment of human keratinocytes in culture with $1,25(OH)_2D_3$ upregulated mRNA for XPC and DDB2 [114]. In an earlier study, both XPC and DDB2 protein levels were significantly increased in human skin biopsies treated topically with $1,25(OH)_2D_3$ at non-UV or UV-irradiated sites [115].

A possible mechanism for the increase in XPC involves phosphatase and tensin homolog deleted on chromosome ten (PTEN). PTEN is tumor suppressor and acts as a negative regulator of the oncogenic acutely transforming retrovirus AKT8 in the rodent T-cell lymphoma (AKT) pathway [116]. It has been reported that UVB down-regulates PTEN in primary human keratinocytes and in mouse skin in an AKT- and extracellular-signal-regulated kinase $(ERK)_{1/2}$-dependent manner [117]. This downregulation of PTEN reduces global genomic NER, through reductions in XPC [118]. More recent studies by Shariev et al. showed that exposure to solar-simulated UV decreased PTEN levels in Skh:hr1 hairless mouse skin [119], as well as primary melanocytes and melanoma cells [120]. The addition of $1,25(OH)_2D_3$ inhibited this UV-induced depletion of PTEN [119], which likely explains the suppression of AKT phosphorylation after UV by $1,25(OH)_2D_3$ [79].

In all this, although vitamin D_3 and lumisterol hydroxyderivatives have been shown to bind to retinoid receptors [71] and to liver X receptors [121], the vitamin D receptor (VDR) in skin and the endoplasmic reticulum protein p57 (ERp57) are clearly key for the reductions in DNA damage by $1,25(OH)_2D_3$ or $24(OH)L_3$. The reductions in both

CPDs and 8-OHdG after UV by either 1,25(OH)$_2$D$_3$ or 24(OH)L$_3$, as well as a CYP11A1 derivative of vitamin D$_3$, 20(OH)D$_3$, were abolished with the knockdown of either ERp57 or VDR [85,122]. VDR-null mice show increased UV-induced DNA damage [123], as well as increased skin tumor formation after UV or chemical carcinogenesis [123,124]. VDR mRNA expression and protein levels were reduced in UVB-irradiated keratinocytes [125]. When human keratinocytes were treated with 24(OH)L$_3$, VDR mRNA and protein levels increased in both UV-irradiated and non-irradiated cells [71].

5. Conclusions

These data collectively indicated that the major over-irradiation metabolite, 24(OH)L$_3$, derived from lumisterol through the actions of CYP11A1 in skin, contributed to the reduction of UV-induced damage in a manner similar to the vitamin D hormone, 1,25(OH)$_2$D$_3$, in keratinocytes and the whole skin. Other CYP11A1 derivatives produced in skin from both vitamin D$_3$ and lumisterol [68,126,127] also reduced UV-induced DNA damage [71,122,126,128]. These findings are consistent with the proposal that this range of UV-generated, 7-dehydrocholesterol-derived, CYP11A1-produced compounds also help reduce UV-induced DNA damage, which is a key precursor to skin tumor development. This proposal would provide an explanation for the reported observations that mice with a knockout of CYP27B1, which is solely responsible for the production of 1,25(OH)$_2$D$_3$ and so cannot produce 1,25(OH)$_2$D$_3$, nevertheless are not more susceptible to UV-induced skin tumors than wild-type mice [129], whereas VDR knockout mice show much greater susceptibility to UV-induced photocarcinogenesis [123].

Author Contributions: Conceptualization, W.G.M.D.S., B.Y.M., M.S.R. and R.S.M.; methodology, R.S.M., M.S.R., K.M.D., M.S.R. and B.Y.M.; validation, M.S.R., K.M.D. and R.S.M.; formal analysis, W.G.M.D.S., B.Y.M. and M.S.R.; investigation, W.G.M.D.S., B.Y.M., J.H., C.Y. and M.S.R.; resources, A.J.A.H., H.S., E.K.Y.T. and R.C.T.; data curation, W.G.M.D.S., B.Y.M. and M.S.R.; writing—original draft preparation, W.G.M.D.S. and B.Y.M.; writing—review and editing, J.H., A.J.A.H., K.M.D., E.K.Y.T., R.C.T., M.S.R. and R.S.M.; visualization, W.G.M.D.S. and B.Y.M.; supervision, M.S.R. and R.S.M.; project administration, W.G.M.D.S., M.S.R. and R.S.M.; funding acquisition, R.S.M. and R.C.T. All authors have read and agreed to the published version of the manuscript.

Funding: The research was funded by the National Health and Medical Research Council of Australia (grant no. APP1070688) and by the Australian Research Council (ARC Linkage grant with Ultraceuticals Pty Ltd. LP100200680).

Institutional Review Board Statement: The study was conducted in accordance with the Declaration of Helsinki and was approved by the Human Research Ethics Committee of the University of Sydney (protocol no. 2015/063).

Informed Consent Statement: Informed consent was obtained from all subjects or parents/guardians involved in the study.

Data Availability Statement: The data that support the findings of this study are available from the corresponding author upon reasonable request. Some data may not be made available because of privacy or ethical restrictions.

Acknowledgments: The authors would like to acknowledge the expert assistance of The Bosch Advanced Microscopy Facility and the Bosch Molecular Biology Facility at the University of Sydney. The authors acknowledge the technical assistance provided by the Sydney Informatics Hub, a Core Research Facility of the University of Sydney.

Conflicts of Interest: The authors declare no conflict of interest. The funders had no role in the design of the study; in the collection, analyses, or interpretation of data; in the writing of the manuscript; or in the decision to publish the results.

References

1. Urbach, F.; Forbes, P.D.; Davies, R.E.; Berger, D. Cutaneous Photobiology: Past, Present and Future. *J. Investig. Dermatol.* **1976**, *67*, 209–224. [CrossRef] [PubMed]
2. Ichihashi, M.; Ueda, M.; Budiyanto, A.; Bito, T.; Oka, M.; Fukunaga, M.; Tsuru, K.; Horikawa, T. UV-induced skin damage. *Toxicology* **2003**, *189*, 21–39. [CrossRef] [PubMed]
3. Beukers, R.; Berends, W. Isolation and identification of the irradiation product of thymine. *Biochim. Biophys. Acta* **1960**, *41*, 550–551. [CrossRef] [PubMed]
4. Halliday, G.M.; Byrne, S.N.; Damian, D.L. Ultraviolet A radiation: Its role in immunosuppression and carcinogenesis. *Semin. Cutan. Med. Surg.* **2011**, *30*, 214–221. [CrossRef]
5. Matsumura, Y.; Ananthaswamy, H.N. Short-term and long-term cellular and molecular events following UV irradiation of skin: Implications for molecular medicine. *Expert Rev. Mol. Med.* **2004**, *4*, 1–22. [CrossRef]
6. Amaro-Ortiz, A.; Yan, B.; D'Orazio, J.A. Ultraviolet radiation, aging and the skin: Prevention of damage by topical cAMP manipulation. *Molecules* **2014**, *19*, 6202–6219. [CrossRef]
7. Yaar, M.; Gilchrest, B.A. Photoageing: Mechanism, prevention and therapy. *Br. J. Dermatol.* **2007**, *157*, 874–887. [CrossRef]
8. Setlow, R.B.; Carrier, W.L. Identification of Ultraviolet-Induced Thymine Dimers in DNA by Absorbance Measurements. *Photochem. Photobiol.* **1963**, *2*, 49–57. [CrossRef]
9. Douki, T.; Court, M.; Sauvaigo, S.; Odin, F.; Cadet, J. Formation of the Main UV-induced Thymine Dimeric Lesions within Isolated and Cellular DNA as Measured by High Performance Liquid Chromatography-Tandem Mass Spectrometry. *J. Biol. Chem.* **2000**, *275*, 11678–11685. [CrossRef]
10. Nakagawa, A.; Kobayashi, N.; Muramatsu, T.; Yamashina, Y.; Shirai, T.; Hashimoto, M.W.; Ikenaga, M.; Mori, T. Three-Dimensional Visualization of Ultraviolet-Induced DNA Damage and Its Repair in Human Cell Nuclei. *J. Investig. Dermatol.* **1998**, *110*, 143–148. [CrossRef]
11. Ames, B.N.; Gold, L.S. Endogenous mutagens and the causes of aging and cancer. *Mutat. Res. Fundam. Mol. Mech. Mutagen.* **1991**, *250*, 3–16. [CrossRef] [PubMed]
12. Ames, B.N. Dietary carcinogens and anticarcinogens. Oxygen radicals and degenerative diseases. *Science* **1983**, *221*, 1256–1263. [CrossRef] [PubMed]
13. Harman, D. Aging: A theory based on free radical and radiation chemistry. *J. Gerontol.* **1956**, *11*, 298–300. [CrossRef] [PubMed]
14. Kvam, E.; Tyrrell, R.M. Induction of oxidative DNA base damage in human skin cells by UV and near visible radiation. *Carcinogenesis* **1997**, *18*, 2379–2384. [CrossRef] [PubMed]
15. Fridovich, I. Biological effects of the superoxide radical. *Arch. Biochem. Biophys.* **1986**, *247*, 1–11. [CrossRef]
16. McAndrew, J.; Patel, R.P.; Jo, H.; Cornwell, T.; Lincoln, T.; Moellering, D.; White, C.R.; Matalon, S.; Darley-Usmar, V. The interplay of nitric oxide and peroxynitrite with signal transduction pathways: Implications for disease. *Semin. Perinatol.* **1997**, *21*, 351–366. [CrossRef]
17. Leccia, M.T.; Yaar, M.; Allen, N.; Gleason, M.; Gilchrest, B.A. Solar simulated irradiation modulates gene expression and activity of antioxidant enzymes in cultured human dermal fibroblasts. *Exp. Dermatol.* **2001**, *10*, 272–279. [CrossRef]
18. Podda, M.; Traber, M.G.; Weber, C.; Yan, L.-J.; Packer, L. UV-Irradiation Depletes Antioxidants and Causes Oxidative Damage in a Model of Human Skin. *Free Radic. Biol. Med.* **1998**, *24*, 55–65. [CrossRef]
19. Van Loon, B.; Markkanen, E.; Hübscher, U. Oxygen as a friend and enemy: How to combat the mutational potential of 8-oxo-guanine. *DNA Repair* **2010**, *9*, 604–616. [CrossRef]
20. Sander, C.S.; Chang, H.; Salzmann, S.; Müller, C.S.L.; Ekanayake-Mudiyanselage, S.; Elsner, P.; Thiele, J.J. Photoaging is Associated with Protein Oxidation in Human Skin In Vivo. *J. Investig. Dermatol.* **2002**, *118*, 618–625. [CrossRef]
21. Fubini, B.; Hubbard, A. Reactive oxygen species (ROS) and reactive nitrogen species (RNS) generation by silica in inflammation and fibrosis. *Free Radic. Biol. Med.* **2003**, *34*, 1507–1516. [CrossRef] [PubMed]
22. Dizdaroglu, M. Oxidative damage to DNA in mammalian chromatin. *Mutat. Res. DNAging* **1992**, *275*, 331–342. [CrossRef] [PubMed]
23. Agnez-Lima, L.F.; Melo, J.T.A.; Silva, A.E.; Oliveira, A.H.S.; Timoteo, A.R.S.; Lima-Bessa, K.M.; Martinez, G.R.; Medeiros, M.H.G.; Di Mascio, P.; Galhardo, R.S.; et al. DNA damage by singlet oxygen and cellular protective mechanisms. *Mutat. Res. Rev. Mutat. Res.* **2012**, *751*, 15–28. [CrossRef] [PubMed]
24. Cadet, J.; Treoule, R. Comparative study of oxidation of nucleic acid components by hydroxyl radicals, singlet oxygen and superoxide anion radicals. *Photochem. Photobiol.* **1978**, *28*, 661–667. [CrossRef]
25. Hallett, F.R.; Hallett, B.P.; Snipes, W. Reactions between Singlet Oxygen and the Constituents of Nucleic Acids: Importance of Reactions in Photodynamic Processes. *Biophys. J.* **1970**, *10*, 305–315. [CrossRef]
26. Kasai, H.; Crain, P.F.; Kuchino, Y.; Nishimura, S.; Ootsuyama, A.; Tanooka, H. Formation of 8-hydroxyguanine moiety in cellular DNA by agents producing oxygen radicals and evidence for its repair. *Carcinogenesis* **1986**, *7*, 1849–1851. [CrossRef]
27. Kasai, H.; Nishimura, S. Hydroxylation of deoxyguanosine at the C-8 position by ascorbic acid and other reducing agents. *Nucleic Acids Res.* **1984**, *12*, 2137–2145. [CrossRef]
28. Hei, T.K.; Liu, S.X.; Waldren, C. Mutagenicity of arsenic in mammalian cells: Role of reactive oxygen species. *Proc. Natl. Acad. Sci. USA* **1998**, *95*, 8103–8107. [CrossRef]

29. Lynn, S.; Gurr, J.-R.; Lai, H.-T.; Jan, K.-Y. NADH Oxidase Activation Is Involved in Arsenite-Induced Oxidative DNA Damage in Human Vascular Smooth Muscle Cells. *Circ. Res.* **2000**, *86*, 514–519. [CrossRef]
30. Simm, A.; Brömme, H.-J. Reactive oxygen species (ROS) and aging: Do we need them—Can we measure them—Should we block them? *Signal Transduct.* **2005**, *5*, 115–125. [CrossRef]
31. Birch-Machin, M.A.; Swalwell, H. How mitochondria record the effects of UV exposure and oxidative stress using human skin as a model tissue. *Mutagenesis* **2010**, *25*, 101–107. [CrossRef] [PubMed]
32. Bosch, R.; Philips, N.; Suárez-Pérez, J.; Juarranz, A.; Devmurari, A.; Chalensouk-Khaosaat, J.; González, S. Mechanisms of Photoaging and Cutaneous Photocarcinogenesis, and Photoprotective Strategies with Phytochemicals. *Antioxidants* **2015**, *4*, 248. [CrossRef] [PubMed]
33. Ogura, R.; Sugiyama, M.; Nishi, J.; Haramaki, N. Mechanism of Lipid Radical Formation Following Exposure of Epidermal Homogenate to Ultraviolet Light. *J. Investig. Dermatol.* **1991**, *97*, 1044–1047. [CrossRef] [PubMed]
34. Bau, D.T.; Gurr, J.R.; Jan, K.Y. Nitric oxide is involved in arsenite inhibition of pyrimidine dimer excision. *Carcinogenesis* **2001**, *22*, 709–716. [CrossRef] [PubMed]
35. Feig, D.I.; Reid, T.M.; Loeb, L.A. Reactive Oxygen Species in Tumorigenesis. *Cancer Res.* **1994**, *54*, 1890s–1894s. [PubMed]
36. De Laat, W.L.; Jaspers, N.G.J.; Hoeijmakers, J.H.J. Molecular mechanism of nucleotide excision repair. *Genes Dev.* **1999**, *13*, 768–785. [CrossRef]
37. Hansson, J.; Munn, M.; Rupp, W.D.; Kahn, R.; Wood, R.D. Localization of DNA repair synthesis by human cell extracts to a short region at the site of a lesion. *J. Biol. Chem.* **1989**, *264*, 21788–21792. [CrossRef]
38. Marteijn, J.A.; Lans, H.; Vermeulen, W.; Hoeijmakers, J.H.J. Understanding nucleotide excision repair and its roles in cancer and ageing. *Nat. Rev. Mol. Cell Biol.* **2014**, *15*, 465–481. [CrossRef]
39. Zotter, A.; Luijsterburg, M.S.; Warmerdam, D.O.; Ibrahim, S.; Nigg, A.; Van Cappellen, W.A.; Hoeijmakers, J.H.J.; Van Driel, R.; Vermeulen, W.; Houtsmuller, A.B. Recruitment of the Nucleotide Excision Repair Endonuclease XPG to Sites of UV-Induced DNA Damage Depends on Functional TFIIH. *Mol. Cell. Biol.* **2006**, *26*, 8868–8879. [CrossRef]
40. Costa, R.M.A.; Chiganças, V.; Da Silva Galhardo, R.; Carvalho, H.; Menck, C.F.M. The eukaryotic nucleotide excision repair pathway. *Biochimie* **2003**, *85*, 1083–1099. [CrossRef]
41. Aboussekhra, A.; Biggerstaff, M.; Shivji, M.K.K.; Vilpo, J.A.; Moncollin, V.; Podust, V.N.; Protić, M.; Hübscher, U.; Egly, J.-M.; Wood, R.D. Mammalian DNA nucleotide excision repair reconstituted with purified protein components. *Cell* **1995**, *80*, 859–868. [CrossRef] [PubMed]
42. Sugasawa, K.; Okamoto, T.; Shimizu, Y.; Masutani, C.; Iwai, S.; Hanaoka, F. A multistep damage recognition mechanism for global genomic nucleotide excision repair. *Genes Dev.* **2001**, *15*, 507–521. [CrossRef] [PubMed]
43. Sugasawa, K.; Ng, J.M.Y.; Masutani, C.; Iwai, S.; Van der Spek, P.J.; Eker, A.P.M.; Hanaoka, F.; Bootsma, D.; Hoeijmakers, J.H.J. Xeroderma Pigmentosum Group C Protein Complex Is the Initiator of Global Genome Nucleotide Excision Repair. *Mol. Cell* **1998**, *2*, 223–232. [CrossRef]
44. Van Cuijk, L.; Vermeulen, W.; Marteijn, J.A. Ubiquitin at work: The ubiquitous regulation of the damage recognition step of NER. *Exp. Cell Res.* **2014**, *329*, 101–109. [CrossRef] [PubMed]
45. Naegeli, H.; Sugasawa, K. The xeroderma pigmentosum pathway: Decision tree analysis of DNA quality. *DNA Repair* **2011**, *10*, 673–683. [CrossRef]
46. Ikegami, T.; Kuraoka, I.; Saijo, M.; Kodo, N.; Kyogoku, Y.; Morikawa, K.; Tanaka, K.; Shirakawa, M. Solution structure of the DNA- and RPA-binding domain of the human repair factor XPA. *Nat. Struct. Mol. Biol.* **1998**, *5*, 701. [CrossRef]
47. Fadda, E. Role of the XPA protein in the NER pathway: A perspective on the function of structural disorder in macromolecular assembly. *Comput. Struct. Biotechnol. J.* **2016**, *14*, 78–85. [CrossRef]
48. Holick, M.F. The Cutaneous Photosynthesis of Previtamin D3: A Unique Photoendocrine System. *J. Investig. Dermatol.* **1981**, *77*, 51–58. [CrossRef]
49. Bikle, D.D.; Nemanic, M.K.; Gee, E.; Elias, P. 1,25-Dihydroxyvitamin D3 production by human keratinocytes. Kinetics and regulation. *J. Clin. Investig.* **1986**, *78*, 557–566. [CrossRef]
50. Bikle, D.D.; Nemanic, M.K.; Whitney, J.O.; Elias, P.W. Neonatal human foreskin keratinocytes produce 1,25-dihydroxyvitamin D3. *Biochemistry* **1986**, *25*, 1545–1548. [CrossRef]
51. Lehmann, B.; Sauter, W.; Knuschke, P.; Dreßler, S.; Meurer, M. Demonstration of UVB-induced synthesis of 1α,25-dihydroxyvitamin D3 (calcitriol) in human skin by microdialysis. *Arch. Dermatol. Res.* **2003**, *295*, 24–28. [CrossRef] [PubMed]
52. Dixon, K.M.; Deo, S.S.; Wong, G.; Slater, M.; Norman, A.W.; Bishop, J.E.; Posner, G.H.; Ishizuka, S.; Halliday, G.M.; Reeve, V.E.; et al. Skin cancer prevention: A possible role of 1,25dihydroxyvitamin D3 and its analogs. *J. Steroid Biochem. Mol. Biol.* **2005**, *97*, 137–143. [CrossRef] [PubMed]
53. Dixon, K.M.; Norman, A.W.; Sequeira, V.B.; Mohan, R.; Rybchyn, M.S.; Reeve, V.E.; Halliday, G.M.; Mason, R.S. 1α,25(OH)2-Vitamin D and a Nongenomic Vitamin D Analogue Inhibit Ultraviolet Radiation–Induced Skin Carcinogenesis. *Cancer Prev. Res.* **2011**, *4*, 1485–1494. [CrossRef] [PubMed]
54. Gordon-Thomson, C.; Gupta, R.; Tongkao-on, W.; Ryan, A.; Halliday, G.M.; Mason, R.S. 1[small alpha],25 Dihydroxyvitamin D3 enhances cellular defences against UV-induced oxidative and other forms of DNA damage in skin. *Photochem. Photobiol. Sci.* **2012**, *11*, 1837–1847. [CrossRef]

55. Gupta, R.; Dixon, K.M.; Deo, S.S.; Holliday, C.J.; Slater, M.; Halliday, G.M.; Reeve, V.E.; Mason, R.S. Photoprotection by 1,25 dihydroxyvitamin D3 is associated with an increase in p53 and a decrease in nitric oxide products. *J. Investig. Derm.* **2007**, *127*, 707–715. [CrossRef]
56. Song, E.J.; Gordon-Thomson, C.; Cole, L.; Stern, H.; Halliday, G.M.; Damian, D.L.; Reeve, V.E.; Mason, R.S. 1α,25-Dihydroxyvitamin D3 reduces several types of UV-induced DNA damage and contributes to photoprotection. *J. Steroid Biochem. Mol. Biol.* **2013**, *136*, 131–138. [CrossRef]
57. Kim, J.S.; Jung, M.; Yoo, J.; Choi, E.H.; Park, B.C.; Kim, M.H.; Hong, S.P. Protective Effect of Topical Vitamin D(3) against Photocarcinogenesis in a Murine Model. *Ann. Dermatol.* **2016**, *28*, 304–313. [CrossRef]
58. Geldenhuys, S.; Hart, P.H.; Endersby, R.; Jacoby, P.; Feelisch, M.; Weller, R.B.; Matthews, V.; Gorman, S. Ultraviolet Radiation Suppresses Obesity and Symptoms of Metabolic Syndrome Independently of Vitamin D in Mice Fed a High-Fat Diet. *Diabetes* **2014**, *63*, 3759–3769. [CrossRef]
59. Weller, R.B. The health benefits of UV radiation exposure through vitamin D production or non-vitamin D pathways. Blood pressure and cardiovascular disease. *Photochem. Photobiol. Sci.* **2017**, *16*, 374–380. [CrossRef]
60. Teng, S.; Chakravorty, L.; Fleury, N.; Gorman, S. Regular exposure to non-burning ultraviolet radiation reduces signs of non-alcoholic fatty liver disease in mature adult mice fed a high fat diet: Results of a pilot study. *BMC Res. Notes* **2019**, *12*, 78. [CrossRef]
61. Havinga, E.; Bots, J.P.L. Studies on vitamin D, I. the synthesis of vitamin D3 3 C14. *Recl. Trav. Chim. Pays-Bas* **1954**, *73*, 393–400. [CrossRef]
62. Heilbron, I.M.; Spring, F.S.; Stewart, P.A. 289. Studies in the sterol group. Part XXI. Lumisterol. *J. Chem. Soc.* **1935**, 1221–1223. [CrossRef]
63. Gottfried, N.; Kaiser, W.; Braun, M.; Fuss, W.; Kompa, K.L. Ultrafast electrocyclic ring opening in previtamin D photochemistry. *Chem. Phys. Lett.* **1984**, *110*, 335–339. [CrossRef]
64. Jacobs, H.J.C.; Havinga, E. Photochemistry of Vitamin D and its Isomers and of Simple Trienes. In *Advances in Photochemistry*; Pitts, J.N., Jr., Hammond, G.S., Gollnick, K., Grosjean, D., Eds.; John Wiley & Sons, Inc.: Hoboken, NJ, USA, 1979; Volume 11, pp. 305–373.
65. Omura, T.; Sato, R. A New Cytochrome in Liver Microsomes. *J. Biol. Chem.* **1962**, *237*, PC1375–PC1376. [CrossRef]
66. Skobowiat, C.; Dowdy, J.C.; Sayre, R.M.; Tuckey, R.C.; Slominski, A. Cutaneous hypothalamic-pituitary-adrenal axis homolog: Regulation by ultraviolet radiation. *Am. J. Physiol. Endocrinol. Metab.* **2011**, *301*, E484–E493. [CrossRef] [PubMed]
67. Slominski, A.T.; Kim, T.-K.; Li, W.; Yi, A.-K.; Postlethwaite, A.; Tuckey, R.C. The role of CYP11A1 in the production of vitamin D metabolites and their role in the regulation of epidermal functions. *J. Steroid Biochem. Mol. Biol.* **2014**, *144*, 28–39. [CrossRef] [PubMed]
68. Tuckey, R.C.; Slominski, A.T.; Cheng, C.Y.S.; Chen, J.; Kim, T.-K.; Xiao, M.; Li, W. Lumisterol is metabolized by CYP11A1: Discovery of a new pathway. *Int. J. Biochem. Cell Biol.* **2014**, *55*, 24–34. [CrossRef]
69. Tuckey, R.C.; Li, W.; Ma, D.; Cheng, C.Y.S.; Wang, K.M.; Kim, T.K.; Jeayeng, S.; Slominski, A.T. CYP27A1 acts on the pre-vitamin D3 photoproduct, lumisterol, producing biologically active hydroxy-metabolites. *J. Steroid Biochem. Mol. Biol.* **2018**, *181*, 1–10. [CrossRef]
70. Tongkao-on, W.; Carter, S.; Reeve, V.E.; Dixon, K.M.; Gordon-Thomson, C.; Halliday, G.M.; Tuckey, R.C.; Mason, R.S. CYP11A1 in skin: An alternative route to photoprotection by vitamin D compounds. *J. Steroid Biochem. Mol. Biol.* **2015**, *148*, 72–78. [CrossRef]
71. Chaiprasongsuk, A.; Janjetovic, Z.; Kim, T.-K.; Schwartz, C.J.; Tuckey, R.; Tang, E.; Raman, C.; Panich, U.; Slominski, A. Hydroxylumisterols, Photoproducts of Pre-Vitamin D3, Protect Human Keratinocytes against UVB-Induced Damage. *Int. J. Mol. Sci.* **2020**, *21*, 9374. [CrossRef]
72. Slominski, A.T.; Kim, T.-K.; Hobrath, J.V.; Janjetovic, Z.; Oak, A.S.W.; Postlethwaite, A.; Lin, Z.; Li, W.; Takeda, Y.; Jetten, A.M.; et al. Characterization of a new pathway that activates lumisterol in vivo to biologically active hydroxylumisterols. *Sci. Rep.* **2017**, *7*, 11434. [CrossRef] [PubMed]
73. Slominski, A.T.; Li, W.; Kim, T.-K.; Semak, I.; Wang, J.; Zjawiony, J.K.; Tuckey, R.C. Novel activities of CYP11A1 and their potential physiological significance. *J. Steroid Biochem. Mol. Biol.* **2015**, *151*, 25–37. [CrossRef] [PubMed]
74. Tuckey, R.C.; Tang, E.K.Y.; Chen, Y.A.; Slominski, A.T. Selective ability of rat 7-Dehydrocholesterol reductase (DHCR7) to act on some 7-Dehydrocholesterol metabolites but not on lumisterol metabolites. *J. Steroid Biochem. Mol. Biol.* **2021**, *212*, 105929. [CrossRef] [PubMed]
75. Dissanayake, N.S.; Greenoak, G.E.; Mason, R.S. Effects of ultraviolet irradiation on human skin-derived epidermal cells in vitro. *J. Cell Physiol.* **1993**, *157*, 119–127. [CrossRef] [PubMed]
76. Sequeira, V.B.; Rybchyn, M.S.; Gordon-Thomson, C.; Tongkao-on, W.; Mizwicki, M.T.; Norman, A.W.; Reeve, V.E.; Halliday, G.M.; Mason, R.S. Opening of Chloride Channels by 1[alpha],25-Dihydroxyvitamin D3 Contributes to Photoprotection against UVR-Induced Thymine Dimers in Keratinocytes. *J. Investig. Derm.* **2013**, *133*, 776–782. [CrossRef]
77. Aasen, T.; Izpisua Belmonte, J.C. Isolation and cultivation of human keratinocytes from skin or plucked hair for the generation of induced pluripotent stem cells. *Nat. Protoc.* **2010**, *5*, 371–382. [CrossRef]
78. McLeod, S.D.; Smith, C.; Mason, R.S. Stimulation of tyrosinase in human melanocytes by pro-opiomelanocortin-derived peptides. *J. Endocrinol.* **1995**, *146*, 439–447. [CrossRef]

79. Rybchyn, M.S.; De Silva, W.G.M.; Sequeira, V.B.; McCarthy, B.Y.; Dilley, A.V.; Dixon, K.M.; Halliday, G.M.; Mason, R.S. Enhanced repair of UV-induced DNA damage by 1,25-Dihydroxyvitamin D3 in skin is linked to pathways that control cellular energy. *J. Investig. Dermatol.* **2018**, *138*, 1146–1156. [CrossRef]
80. Tuckey, R.C.; Li, W.; Zjawiony, J.K.; Zmijewski, M.A.; Nguyen, M.N.; Sweatman, T.; Miller, D.; Slominski, A. Pathways and products for the metabolism of vitamin D3 by cytochrome P450scc. *FEBS J.* **2008**, *275*, 2585–2596. [CrossRef]
81. Cooke, M.S.; Robson, A. Immunochemical detection of UV-induced DNA damage and repair. *Methods Mol. Biol.* **2006**, *314*, 215–228. [CrossRef]
82. Mouret, S.; Baudouin, C.; Charveron, M.; Favier, A.; Cadet, J.; Douki, T. Cyclobutane pyrimidine dimers are predominant DNA lesions in whole human skin exposed to UVA radiation. *Proc. Natl. Acad. Sci. USA* **2006**, *103*, 13765–13770. [CrossRef] [PubMed]
83. Wong, G.; Gupta, R.; Dixon, K.M.; Deo, S.S.; Choong, S.M.; Halliday, G.M.; Bishop, J.E.; Ishizuka, S.; Norman, A.W.; Posner, G.H.; et al. 1,25-Dihydroxyvitamin D and three low-calcemic analogs decrease UV-induced DNA damage via the rapid response pathway. *J. Steroid Biochem. Mol. Biol.* **2004**, *89–90*, 567–570. [CrossRef] [PubMed]
84. Ohno, M.; Miura, T.; Furuichi, M.; Tominaga, Y.; Tsuchimoto, D.; Sakumi, K.; Nakabeppu, Y. A genome-wide distribution of 8-oxoguanine correlates with the preferred regions for recombination and single nucleotide polymorphism in the human genome. *Genome Res.* **2006**, *16*, 567–575. [CrossRef] [PubMed]
85. Sequeira, V.B.; Rybchyn, M.S.; Tongkao-On, W.; Gordon-Thomson, C.; Malloy, P.J.; Nemere, I.; Norman, A.W.; Reeve, V.E.; Halliday, G.M.; Feldman, D.; et al. The role of the vitamin D receptor and ERp57 in photoprotection by 1alpha,25-dihydroxyvitamin D3. *Mol. Endocrinol.* **2012**, *26*, 574–582. [CrossRef]
86. Hönigsmann, H.; Brenner, W.; Tanew, A.; Ortel, B. UV-Induced unscheduled DNA synthesis in human skin: Dose response, correlation with erythema, time course and split dose exposure in vivo. *J. Photochem. Photobiol. B Biol.* **1987**, *1*, 33–43. [CrossRef]
87. Pieper, A.A.; Verma, A.; Zhang, J.; Snyder, S.H. Poly (ADP-ribose) polymerase, nitric oxide and cell death. *Trends Pharmacol. Sci.* **1999**, *20*, 171–181. [CrossRef]
88. Tettamanti, G.; Malagoli, D.; Ottaviani, E.; De Eguileor, M. Oligomycin A and the IPLB-LdFB insect cell line: Actin and mitochondrial responses. *Cell Biol. Int.* **2008**, *32*, 287–292. [CrossRef]
89. Tettamanti, G.; Malagoli, D.; Marchesini, E.; Congiu, T.; De Eguileor, M.; Ottaviani, E. Oligomycin A induces autophagy in the IPLB-LdFB insect cell line. *Cell Tissue Res.* **2006**, *326*, 179–186. [CrossRef]
90. Zhang, D.; Li, J.; Wang, F.; Hu, J.; Wang, S.; Sun, Y. 2-Deoxy-D-glucose targeting of glucose metabolism in cancer cells as a potential therapy. *Cancer Lett.* **2014**, *355*, 176–183. [CrossRef]
91. Wiseman, H.; Halliwell, B. Damage to DNA by reactive oxygen and nitrogen species: Role in inflammatory disease and progression to cancer. *Biochem. J.* **1996**, *313 Pt 1*, 17–29. [CrossRef]
92. Rybchyn, M.S.; Brennan-Speranza, T.C.; Mor, D.; Cheng, Z.; Chang, W.; Conigrave, A.D.; Mason, R.S. The mTORC2 Regulator Homer1 Modulates Protein Levels and Sub-Cellular Localization of the CaSR in Osteoblast-Lineage Cells. *Int. J. Mol. Sci.* **2021**, *22*, 6509. [CrossRef] [PubMed]
93. Dixon, K.M.; Deo, S.S.; Norman, A.W.; Bishop, J.E.; Halliday, G.M.; Reeve, V.E.; Mason, R.S. In vivo relevance for photoprotection by the vitamin D rapid response pathway. *J. Steroid Biochem. Mol. Biol.* **2007**, *103*, 451–456. [CrossRef] [PubMed]
94. De Haes, P.; Garmyn, M.; Verstuyf, A.; De Clercq, P.; Vandewalle, M.; Degreef, H.; Vantieghem, K.; Bouillon, R.; Segaert, S. 1,25-Dihydroxyvitamin D3 and analogues protect primary human keratinocytes against UVB-induced DNA damage. *J. Photochem. Photobiol. B Biol.* **2005**, *78*, 141–148. [CrossRef] [PubMed]
95. Slominski, A.T.; Janjetovic, Z.; Kim, T.-K.; Wasilewski, P.; Rosas, S.; Hanna, S.; Sayre, R.M.; Dowdy, J.C.; Li, W.; Tuckey, R.C. Novel non-calcemic secosteroids that are produced by human epidermal keratinocytes protect against solar radiation. *J. Steroid Biochem. Mol. Biol.* **2015**, *148*, 52–63. [CrossRef] [PubMed]
96. Beyer, R.E. The effect of ultraviolet light on mitochondria. I. Inactivation and protection of oxidative phosphorylation during far-ultraviolet irradiation. *Arch. Biochem. Biophys.* **1959**, *79*, 269–274. [CrossRef]
97. Maglio, D.H.G.; Paz, M.L.; Ferrari, A.; Weill, F.S.; Czerniczyniec, A.; Leoni, J.; Bustamante, J. Skin damage and mitochondrial dysfunction after acute ultraviolet B irradiation: Relationship with nitric oxide production. *Photodermatol. Photoimmunol. Photomed.* **2005**, *21*, 311–317. [CrossRef]
98. Scherz-Shouval, R.; Elazar, Z. Regulation of autophagy by ROS: Physiology and pathology. *Trends Biochem. Sci.* **2011**, *36*, 30–38. [CrossRef]
99. Ravikumar, B.; Sarkar, S.; Davies, J.E.; Futter, M.; Garcia-Arencibia, M.; Green-Thompson, Z.W.; Jimenez-Sanchez, M.; Korolchuk, V.I.; Lichtenberg, M.; Luo, S.; et al. Regulation of Mammalian Autophagy in Physiology and Pathophysiology. *Physiol. Rev.* **2010**, *90*, 1383–1435. [CrossRef]
100. Li, Z.-Y.; Yang, Y.; Ming, M.; Liu, B. Mitochondrial ROS generation for regulation of autophagic pathways in cancer. *Biochem. Biophys. Res. Commun.* **2011**, *414*, 5–8. [CrossRef]
101. McLelland, G.L.; Soubannier, V.; Chen, C.X.; McBride, H.M.; Fon, E.A. Parkin and PINK1 function in a vesicular trafficking pathway regulating mitochondrial quality control. *EMBO J.* **2014**, *33*, 282–295. [CrossRef]
102. Gezen-Ak, D.; Alaylıoğlu, M.; Yurttaş, Z.; Çamoğlu, T.; Şengül, B.; İşler, C.; Kına, Ü.Y.; Keskin, E.; Atasoy, İ.L.; Kafardar, A.M.; et al. Vitamin D receptor regulates transcription of mitochondrial DNA and directly interacts with mitochondrial DNA and TFAM. *J. Nutr. Biochem.* **2023**, *116*, 109322. [CrossRef] [PubMed]

103. Ricca, C.; Aillon, A.; Bergandi, L.; Alotto, D.; Castagnoli, C.; Silvagno, F. Vitamin D Receptor Is Necessary for Mitochondrial Function and Cell Health. *Int. J. Mol. Sci.* **2018**, *19*, 1672. [CrossRef] [PubMed]
104. Lin, R.; Nagai, Y.; Sladek, R.; Bastien, Y.; Ho, J.; Petrecca, K.; Sotiropoulou, G.; Diamandis, E.P.; Hudson, T.J.; White, J.H. Expression profiling in squamous carcinoma cells reveals pleiotropic effects of vitamin D3 analog EB1089 signaling on cell proliferation, differentiation, and immune system regulation. *Mol. Endocrinol.* **2002**, *16*, 1243–1256. [CrossRef] [PubMed]
105. Nakai, K.; Fujii, H.; Kono, K.; Goto, S.; Kitazawa, R.; Kitazawa, S.; Hirata, M.; Shinohara, M.; Fukagawa, M.; Nishi, S. Vitamin D activates the Nrf2-Keap1 antioxidant pathway and ameliorates nephropathy in diabetic rats. *Am. J. Hypertens.* **2014**, *27*, 586–595. [CrossRef] [PubMed]
106. Berridge, M.J. Vitamin D cell signalling in health and disease. *Biochem. Biophys. Res. Commun.* **2015**, *460*, 53–71. [CrossRef]
107. Chaiprasongsuk, A.; Janjetovic, Z.; Kim, T.-K.; Holick, M.F.; Tuckey, R.C.; Panich, U.; Slominski, A.T. 274—Protective effects of novel derivatives of vitamin D3 and lumisterol against UVB-induced damage in human keratinocytes involve activation of Nrf2 and P53 defense mechanisms. *Free Radic. Biol. Med.* **2019**, *128*, S116. [CrossRef]
108. Slominski, A.T.; Kim, T.-K.; Slominski, R.M.; Song, Y.; Janjetovic, Z.; Podgorska, E.; Reddy, S.B.; Song, Y.; Raman, C.; Tang, E.K.Y.; et al. Metabolic activation of tachysterol3 to biologically active hydroxyderivatives that act on VDR, AhR, LXRs, and PPARγ receptors. *FASEB J.* **2022**, *36*, e22451. [CrossRef]
109. Burney, S.; Caulfield, J.L.; Niles, J.C.; Wishnok, J.S.; Tannenbaum, S.R. The chemistry of DNA damage from nitric oxide and peroxynitrite. *Mutat. Res. Fundam. Mol. Mech. Mutagen.* **1999**, *424*, 37–49. [CrossRef]
110. Jaiswal, M.; LaRusso, N.F.; Burgart, L.J.; Gores, G.J. Inflammatory Cytokines Induce DNA damage and Inhibit DNA repair in Cholangiocarcinoma Cells by a Nitric Oxide-dependent Mechanism. *Cancer Res.* **2000**, *60*, 184–190.
111. Steeg, H.V.; Vries, A.D.; Oostrom, C.T.M.V.; Benthem, J.V.; Beems, R.B.; Kreijl, C.F.V. DNA Repair—Deficient Xpa and Xpa/p53+/− Knock-Out Mice: Nature of the Models. *Toxicol. Pathol.* **2001**, *29*, 109–116. [CrossRef]
112. Volker, M.; Moné, M.J.; Karmakar, P.; Van Hoffen, A.; Schul, W.; Vermeulen, W.; Hoeijmakers, J.H.J.; Van Driel, R.; Van Zeeland, A.A.; Mullenders, L.H.F. Sequential Assembly of the Nucleotide Excision Repair Factors In Vivo. *Mol. Cell* **2001**, *8*, 213–224. [CrossRef] [PubMed]
113. Wang, Q.-E.; Zhu, Q.; Wani, G.; El-Mahdy, M.A.; Li, J.; Wani, A.A. DNA repair factor XPC is modified by SUMO-1 and ubiquitin following UV irradiation. *Nucleic Acids Res.* **2005**, *33*, 4023–4034. [CrossRef] [PubMed]
114. Moll, P.R.; Sander, V.; Frischauf, A.-M.; Richter, K. Expression profiling of vitamin D treated primary human keratinocytes. *J. Cell. Biochem.* **2007**, *100*, 574–592. [CrossRef] [PubMed]
115. Song, E.J.Y. Photoprotection by 1(alpha),25-Dihydroxyvitamin D3 and Vitamin D Like Compound in Human Skin. Master's Thesis, University of Sydney, Sydney, Australia, 2014.
116. Leslie, N.R.; Batty, I.H.; Maccario, H.; Davidson, L.; Downes, C.P. Understanding PTEN regulation: PIP2, polarity and protein stability. *Oncogene* **2008**, *27*, 5464–5476. [CrossRef]
117. Ming, M.; Han, W.; Maddox, J.; Soltani, K.; Shea, C.R.; Freeman, D.M.; He, Y.Y. UVB-induced ERK/AKT-dependent PTEN suppression promotes survival of epidermal keratinocytes. *Oncogene* **2010**, *29*, 492–502. [CrossRef]
118. Ming, M.; Feng, L.; Shea, C.R.; Soltani, K.; Zhao, B.; Han, W.; Smart, R.C.; Trempus, C.S.; He, Y.Y. PTEN positively regulates UVB-induced DNA damage repair. *Cancer Res.* **2011**, *71*, 5287–5295. [CrossRef]
119. Shariev, A. Novel targets for Vitamin D in the Inhibition of Melanoma Growth and Metastasis. Ph.D. Thesis, University of Sydney, Sydney Medical School, Sydney, Australia, 2019.
120. Shariev, A.; Painter, N.; Reeve, V.E.; Haass, N.K.; Rybchyn, M.S.; Ince, F.A.; Mason, R.S.; Dixon, K.M. PTEN: A novel target for vitamin D in melanoma. *J. Steroid Biochem. Mol. Biol.* **2022**, *218*, 106059. [CrossRef]
121. Slominski, A.T.; Kim, T.K.; Qayyum, S.; Song, Y.; Janjetovic, Z.; Oak, A.S.W.; Slominski, R.M.; Raman, C.; Stefan, J.; Mier-Aguilar, C.A.; et al. Vitamin D and lumisterol derivatives can act on liver X receptors (LXRs). *Sci. Rep.* **2021**, *11*, 8002. [CrossRef]
122. De Silva, W.G.M.; Han, J.Z.R.; Yang, C.; Tongkao-On, W.; McCarthy, B.Y.; Ince, F.A.; Holland, A.J.A.; Tuckey, R.C.; Slominski, A.T.; Abboud, M.; et al. Evidence for Involvement of Nonclassical Pathways in the Protection From UV-Induced DNA Damage by Vitamin D–Related Compounds. *JBMR Plus* **2021**, *5*, e10555. [CrossRef]
123. Ellison, T.I.; Smith, M.K.; Gilliam, A.C.; MacDonald, P.N. Inactivation of the Vitamin D Receptor Enhances Susceptibility of Murine Skin to UV-induced Tumorigenesis. *J. Investig. Dermatol.* **2008**, *128*, 2508–2517. [CrossRef]
124. Zinser, G.M.; Sundberg, J.P.; Welsh, J. Vitamin D3 receptor ablation sensitizes skin to chemically induced tumorigenesis. *Carcinogenesis* **2002**, *23*, 2103–2109. [CrossRef] [PubMed]
125. Courtois, S.J.; Segaert, S.; Degreef, H.; Bouillon, R.; Garmyn, M. Ultraviolet B Suppresses Vitamin D Receptor Gene Expression in Keratinocytes. *Biochem. Biophys. Res. Commun.* **1998**, *246*, 64–69. [CrossRef] [PubMed]
126. Slominski, A.T.; Chaiprasongsuk, A.; Janjetovic, Z.; Kim, T.K.; Stefan, J.; Slominski, R.M.; Hanumanthu, V.S.; Raman, C.; Qayyum, S.; Song, Y.; et al. Photoprotective Properties of Vitamin D and Lumisterol Hydroxyderivatives. *Cell Biochem. Biophys.* **2020**, *78*, 165–180. [CrossRef]
127. Slominski, A.T.; Kim, T.K.; Li, W.; Postlethwaite, A.; Tieu, E.W.; Tang, E.K.Y.; Tuckey, R.C. Detection of novel CYP11A1-derived secosteroids in the human epidermis and serum and pig adrenal gland. *Sci. Rep.* **2015**, *5*, 14875. [CrossRef] [PubMed]

128. Tongkao-on, W. Role of Vitamin D and Other Compounds in the Protection of Skin Cells from UV. Ph.D. Thesis, University of Sydney, Sydney, Australia, 2015.
129. Teichert, A.E.; Elalieh, H.; Elias, P.M.; Welsh, J.; Bikle, D.D. Overexpression of hedgehog signaling is associated with epidermal tumor formation in vitamin D receptor-null mice. *J. Investig. Dermatol.* **2011**, *131*, 2289–2297. [CrossRef]

Disclaimer/Publisher's Note: The statements, opinions and data contained in all publications are solely those of the individual author(s) and contributor(s) and not of MDPI and/or the editor(s). MDPI and/or the editor(s) disclaim responsibility for any injury to people or property resulting from any ideas, methods, instructions or products referred to in the content.